

UNIVERSIDADE FEDERAL DO ABC

CAMILA BACCONI ALVES GARCIA

**SISTEMA DE DETERMINAÇÃO DE ATITUDE EMBARCADO NUM
NANOSATÉLITE**

São Bernardo do Campos, SP - Brazil

2016

UNIVERSIDADE FEDERAL DO ABC

TRABALHO DE GRADUAÇÃO
AEROSPACE ENGINEERING

CAMILA BACCONI ALVES GARCIA

ATTITUDE DETERMINATION SYSTEM ON BOARD OF A
NANOSATELLITE

Supervisor: Luiz de Siqueira Martins-Filho
Professor of Aerospace Engineering

Bachelor dissertation submitted to the Center of Engineering, Modelling and Applied Social Sciences (CECS) in partial fulfillment of the requirements for the undergraduate degree in Aerospace Engineering at UFABC.

São Bernardo do Campo, SP - Brazil

2016

Bacconi Alves Garcia, Camila

Sistema de Determinação de Atitude Embarcado num Nanosatélite / Attitude Determination System On Board of a Nanosatellite / Camila Bacconi Alves Garcia. — 2016.

xx fls./p. : il.

Orientador / Supervisor: Luiz de Siqueira Martins Filho

Trabalho de Conclusão de Curso — Universidade Federal do ABC, Bacharelado em Engenharia Aeroespacial, São Bernardo do Campo, 2016.

1. Nanosatellite. 2. Attitude Determination. 3. QUEST. 4. Magnetic Field 5. Sun Position.

CAMILA BACCONI ALVES GARCIA

**ATTITUDE DETERMINATION SYSTEM ON BOARD OF A
NANOSATELLITE**

Bachelor dissertation submitted to the
Center of Engineering, Modelling and
Applied Social Sciences (CECS) in partial
fulfillment of the requirements for the
undergraduate degree in Aerospace
Engineering at UFABC.

APPROVED DISSERTATION

São Bernardo do Campos, August 18th, 2016

Prof. Dr. Luiz de Siqueira Martins-Filho
Supervisor

Prof. Dr. Antonio Gil Vicente de Brum
UFABC

Prof. Dr. Leandro Baroni
UFABC

ACKNOWLEDGEMENT

I would like to thank my supervisor Professor Luiz de Siqueira Martins-Filho (UFABC) for introducing me to the topic as well for supporting me throughout my study and research. In addition, I would like to thank Professor Helio Kuga (INPE) and Professor Valdemir Carrara (INPE) for sharing their knowledge and for clearing my doubts about the code. Finally, but not least, I would like to thank my family and friends for always believing in me.

“In space flight, “attitude” refers to orientation: which direction your vehicle is pointing relative to the Sun, Earth and other spacecraft. If you lose control of your attitude, two things happen: the vehicle starts to tumble and spin, disorienting everyone on board, and it also strays from its course, which, if you’re short on time or fuel, could mean the difference between life and death. In the Soyuz, for example, we use every cue from every available source—periscope, multiple sensors, the horizon—to monitor our attitude constantly and adjust if necessary. We never want to lose attitude, since maintaining attitude is fundamental to success. In my experience, something similar is true on Earth. Ultimately, I don’t determine whether I arrive at the desired professional destination. Too many variables are out of my control. There’s really just one thing I can control: my attitude during the journey, which is what keeps me feeling steady and stable, and what keeps me headed in the right direction. So I consciously monitor and correct, if necessary, because losing attitude would be far worse than not achieving my goal.”

— Chris Hadfield, *An Astronaut's Guide to Life on Earth*

ABSTRACT

This work studies the attitude determination system that will be on board of the nanosatellite NANOSATC-BR2, which is being developed by INPE (Instituto Nacional de Pesquisas Espaciais) and Universidade Federal de Santa Maria (UFSM) in cooperation with other Brazilian universities. The “Sistema de Determinação de Atitude Tolerante à Falhas” (SDTAF), the first attitude determination system developed in Brazil, is result of a cooperation between Universidade Federal de Minas Gerais (UFMG), Universidade Federal do ABC (UFABC) and INPE. The SDTAF will be validated in space through the comparison of its quaternions and the quaternions of the attitude determination system of the NANOSATC-BR2. This system utilizes a magnetometer and solar sensors which provide the attitude using the QUEST algorithm. UFABC is responsible for the study and simulation of the attitude determination software, including the error analysis of mathematical models which determine the magnetic field vector and sun position vector in the inertial frame. The model used to determine the sun position vector was compared with other two models found in literature, and also compared to the outputs given by STK 10. The IGRF12 model truncated for $n=m=5$ was compared to the original model ($n=m=13$). Simulations for different rotation sequences and different Euler Angles were made, and the results of the quaternions are according the expected. Additionally, the sun position vectors in the inertial frame provided an average angle error lower than 1° , and the average magnitude error was approximately 1% in comparison with the models found in literature and in comparison with STK results. Finally, the magnetic field vector in the inertial frame determined using the IGRF12 model for $n=m=5$ provided average angle errors and average magnitude errors lower than 1° and 1%, respectively, when compared with the original model ($n=m=13$).

Keywords: Nanosatellites, Attitude Determination, QUEST, Sun Position, Magnetic Field

RESUMO

Esse trabalho trata do estudo e da análise de erros de um sistema de determinação de atitude a ser embarcado no nanossatélite NANOSATC-BR2, que está sendo desenvolvido pelo Instituto Nacional de Pesquisas Espaciais (INPE) e pela Universidade Federal de Santa Maria (UFSM) em cooperação com outras Universidades brasileiras. Os principais objetivos dessa missão coletar dados do campo magnético terrestre, e testar circuitos integrados desenvolvidos no Brasil. O Sistema de Determinação de Atitude Tolerante à Falhas (SDATF) é o primeiro sistema desenvolvido no Brasil, fruto de uma cooperação entre a Universidade Federal de Minas Gerais (UFMG), Universidade Federal do ABC (UFABC) e o INPE, e ele será validado no espaço através dos resultados dos seus quaternions que serão comparados com os quaternions do sistema de determinação de atitude do NANOSATC-BR2. Esse sistema utiliza como sensores um magnetômetro triaxial, e sensores solares para a determinação da atitude através do algoritmo QUEST. As atividades da UFABC apresentadas nesse trabalho, basearam-se no estudo do software de sistema de determinação de atitude, e na análise de erros dos modelos matemáticos para determinar o vetor de posição do sol e o vetor do campo magnético terrestre no referencial inercial. O modelo do vetor de posição do sol foi com outros modelos encontrados na literatura e com o STK. O modelo IGFR12 truncado em $n=m=5$, utilizado para determinar o campo magnético, foi comparado com o modelo não truncado ($n=m=13$). Simulações para diferentes sequências de rotações e diferentes ângulos de Euler foram feitas e os resultados dos quaternions estão de acordo com o esperado. Adicionalmente, os vetores da posição solar no referencial inercial forneceram erro angular médio menor que 1° e erro médio de magnitude de aproximadamente 1% em relação a outros modelos encontrados na literatura e em relação ao STK. Por fim, o vetor do campo magnético no referencial inercial calculado através do IGRF12 truncado em $n=m=5$ forneceu erros médios angulares e erros médios de magnitude menores do que 1° e 1%, respectivamente.

Palavras-chave: Nanosatélites, Determinação de atitude, QUEST, Posição do Sol, Campo Magnético.

LIST OF FIGURES

LIST OF TABLES

LIST OF ACRONYMS AND ABBREVIATIONS

ADCS	Attitude Determination and Control System
CITAR	Circuitos Integrados Tolerantes a Radiações
ESA	European Space Agency
FINEP	Financiadora de Estudos e Projetos
IGRF	International Geomagnetic Reference Field
INPE	Instituto Nacional de Pesquisas Espaciais
JD	Julian Date
JDS	Julian Date for Space
LABSIM	Laboratório de Simulação
LIT	Laboratório de Integração e Testes
MCT	Ministério da Ciência e Tecnologia
MCTI	Ministério da Ciência, Tecnologia e Inovação
MJD	Modified Julian Date
NASA	National Aeronautics and Space Administration
NORAD	North American Aerospace Defense Command
NIST	National Institute of Standards and Technology
SDATF	Sistema de Determinação de Atitude Tolerante à Falhas
SEE	Single Event Effect
SEB	Single Event Burnout
SEL	Single Event Latchup
SEU	Single Event Upset
STK	Systems Tool Kit
TAI	International Atomic Time
TDT	Terrestrial Dynamical Time
TLE	Two Line Elements
TT	Terrestrial Time
UFABC	Universidade Federal do ABC
UFMG	Universidade Federal de Minas Gerais
UFSC	Universidade Federal de Santa Maria
USSPACECOM	United States Space Command
UT	Universal Time

UTC

Coordinated Universal Time

CONTENTS

1 INTRODUCTION	1
1.1 CUBESATS.....	1
1.2 NANOSATC-BR PROGRAM – DEVELOPMENT OF CUBESATS.....	2
1.2.1 NANOSATC-BR2.....	3
1.3 OBJECTIVES.....	6
2 BACKGROUND INFORMATION	7
2.1 COORDINATE SYSTEMS	7
2.1.1 GEOCENTRIC INERTIAL COORDINATE SYSTEM.....	7
2.1.2 TERRESTRIAL CARTESIAN COORDINATES SYSTEM	7
2.1.3 BODY-FIXED COORDINATE SYSTEM	9
2.3 ATTITUDE DETERMINATION	9
2.3.1 TRIAD	10
2.3.2 QUATERNION	11
2.3.3 Q-METHOD	12
2.3.4 QUEST (QUaternion ESTimator)	14
2.4 ORBITAL ELEMENTS	15
2.4.1 OTHER ORBITAL ELEMENTS.....	19
2.5 TIME MEASUREMENTS.....	24
2.5.1 TYPES OF JULIAN DATES	25
2.5.2 GREENWICH MEAN SIDERAL TIME	27
3 MATHEMATICAL MODELING.....	29
3.1 SUN POSITION VECTOR.....	29
3.1.1 NANOSATC-BR2 MODEL.....	29
3.1.2 DAVID VALLADO’S MODEL	31
3.1.3 ASTRONOMICAL ALMANAC MODEL	33

3.1.4 CONSIDERATIONS.....	34
3.2 MAGNETIC FIELD VECTOR.....	35
3.2.1 MATHEMATICAL MODEL – IGRF12.....	35
3.3 ERROR ANALYSIS	38
4 SOFTWARE ARCHITECTURE.....	39
4.1 TWO-LINE ELEMENT (TLE)	42
4.2 ATTITUDE DETERMINATION	44
5 SIMULATION & ERROR ANALYSIS	49
5.1 SIMULATION RESULTS: ATTITUDE DETERMINATION.....	49
5.1.2 SIMULATION 1	49
5.1.2 SIMULATION 2	52
5.1.3 SIMULATION 3	55
5.2 ERROR ANALYSIS: SUN POSITION VECTOR.....	57
5.2.1 MODIFICATION INTO THE ORIGINAL MODEL	61
5.2 ERROR ANALYSIS: MAGNETIC FIELD VECTOR	63
6 SCHEDULE OF ACTIVITIES.....	66
7 CONCLUSIONS.....	67
REFERENCES	69

1 INTRODUCTION

1.1 CUBESATS

In 1999, Professor Jordi Puig-Suari of the California Polytechnic State University and Professor Bob Twiggs of Stanford University started a project with the aim to standardize the design of a pico nanosatellite in order to reduce costs and development time, increase the space accessibility, and also to become launches more frequent. This project gave birth to what we know today as “Cubesats”. Cubesats are satellites with the format of cubes, as depicted in Figure 1.1 (CubeSat Design Specification, 2014). There are several types of CubeSats, depending on its dimensions. For example, a 1U Cubesat is a Cubesat that have the following dimensions: 10cm x 10cm x 10cm Cubesat. A 3U Cubesat and a 2U Cubesat have the following dimensions, respectively: 10cm x 10cm x 30cm and 10cm x 10cm x 20cm.

This dissertation is related to an attitude determination software that is one of the payloads of the NanoSatC-BR2, which is a 2U Cubesat.

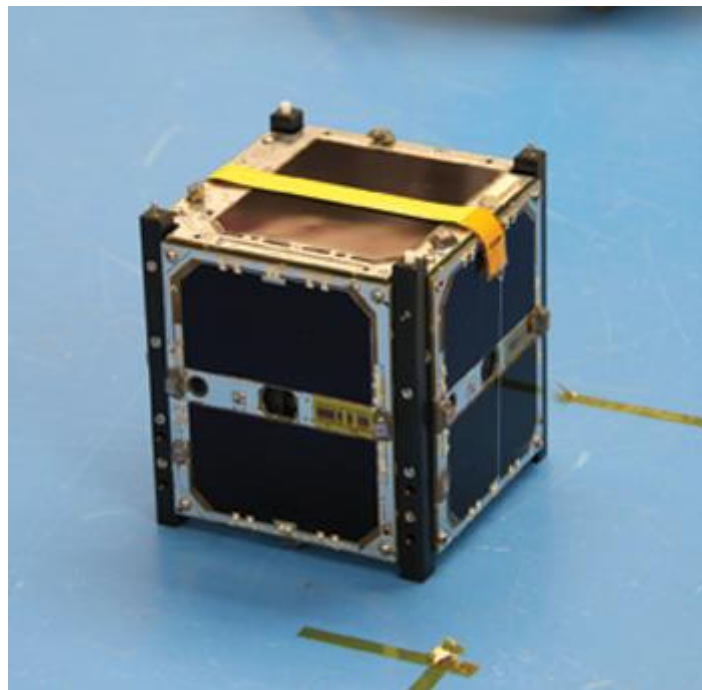


Figure 1.1 – Cubesat MCubed-2 built by students at University of Michigan, USA. Source: Martin, 2013.

According to Maini & Agrawal (2014), the classification of satellites is made based on their total mass (including fuel) as shown in Table 2.1.

Table 2.1 – Classification of Satellites

Class	Massa (kg)
Large Satellite	>1000
Medium Satellite	500-1000
Mini Satellite	100-500
Micro Satellite	10-100
Nano Satellite	1-10
Pico Satellite	0.1-1
Femto Satellite	<0.1

Source: Maini & Agrawal, 2014.

1.2 NANOSATC-BR PROGRAM – DEVELOPMENT OF CUBESATS

The NanosatC-BR2 is a satellite of the “NANOSATC-BR – Development of CubeSats” Program, which is being developed by the National Institute of Space Research (INPE), in São José dos Campos, Brazil, in collaboration with Brazilian Universities. The main objectives of this program are listed below (INPE, 2015):

- Capacitate human resources in the undergraduate level for research and development of space instrumentation, in order to improve the quality and the standard of the undergraduate programs of the participating universities, especially the programs at the Universidade Federal de Santa Maria (UFSM);
- Capacitate technologically the participating institutions, providing development in the areas of science, engineering and space technology;
- Monitor geomagnetic conditions above the regions where Brazil is located, such as regions of the South Atlantic Magnetic Anomaly and the Equatorial Ionospheric Electrojet;
- Qualify miniaturized electronic circuits and integrated circuits of the Project CITAR-FINEP in space;

- Provide scientific research related to the phenomenology of the Geospace and Space Climate, either in space or on the surface above Brazil.

The first satellite of the NanoSatC-BR, a 1U Cubesat entitled NANOSATC-BR1, is already on orbit since 2014. Thus, the NanosatC-BR2 is the second satellite of this program.

1.2.1 NANOSATC-BR2

The mission of the NanosatC-BR2 has the following objectives (Durão & Essado, 2014):

- To collect data of the terrestrial magnetic field, especially in the region of the South America Magnetic Anomaly;
- To test integrated circuits designed in Brazil which are radiation resistant, with the aim to use them in large satellites in the future.

The Flight Model (Fig. 1.2) of the NanosatC-BR2 is at LIT/INPE-MCTI, and its launch is scheduled to happen in the second half of 2016. The Engineering Model (Fig. 1.3) is at LABSIM/ETE/INPE-MCTI, and it is being utilized for tests in its systems and subsystems.



Figure 1.2 – Fight Model of the NanoSatC-BR2 Source: Durão & Essado, 2014

Besides the UFSM, other universities are also participating in this project, such as the Universidade Federal de Minas Gerais (UFMG) and the Universidade Federal do ABC (UFABC). UFABC is responsible for the simulation of the attitude determination software, including the error analysis of algorithms, such as algorithms of the mathematical models that determines the terrestrial magnetic field and sun position vector in the inertial frame.



Figure 1.3 – Engineering Model of the NanoSatC-BR2 (Durão & Essado, 2014)

The *Sistema de Determinação de Atitude Tolerante à Falhas* (SDATF), the first attitude determination system developed in Brazil, is result of a cooperation between UFMG, INPE and UFABC. This is a fault tolerant system to avoid Single Event Effects (SEEs), which is the “disturbance of an active electronic device caused by a single energetic particle”, (Normand, 1998) caused by cosmic rays and high energy protons. These effects can take on many forms, such as Single Event Upset (SEU), Single Event Latchup (SEL) and Single Event Burnout (SEB). SEU “normally appear as transient pulses in logic or support circuitry, or as bitflips in memory cells or registers” (Holbert, 2006). SEU is transient soft errors and non-destructive, which means that a reset of the device results in a properly behavior of the system. SEL is a hard error and potentially destructive, which “results in a high operating current, above device specifications, and must be cleared by a power reset” (Holbert, 2006), and if the power is not reseted, a catastrophic failure can occur due to excessive heating, for example. SEB “can cause the device destruction due to a high current state in a power transistor” (Holbert, 2006), and

consequently it causes the failure of the device permanently. The SDATF is a fault tolerant system developed to avoid SEUs.

The attitude determination system described in the present work is a scientific payload of the NanosatC-BR2, and it is going to be validated in space through the comparison of its results with the results of the attitude determination system of the nanosatellite. The SDATF (Figure 1.4) is an integrated circuit board composed of three microcontrollers, a three axis magnetometer (XEN 1210), resistors, capacitors, etc.

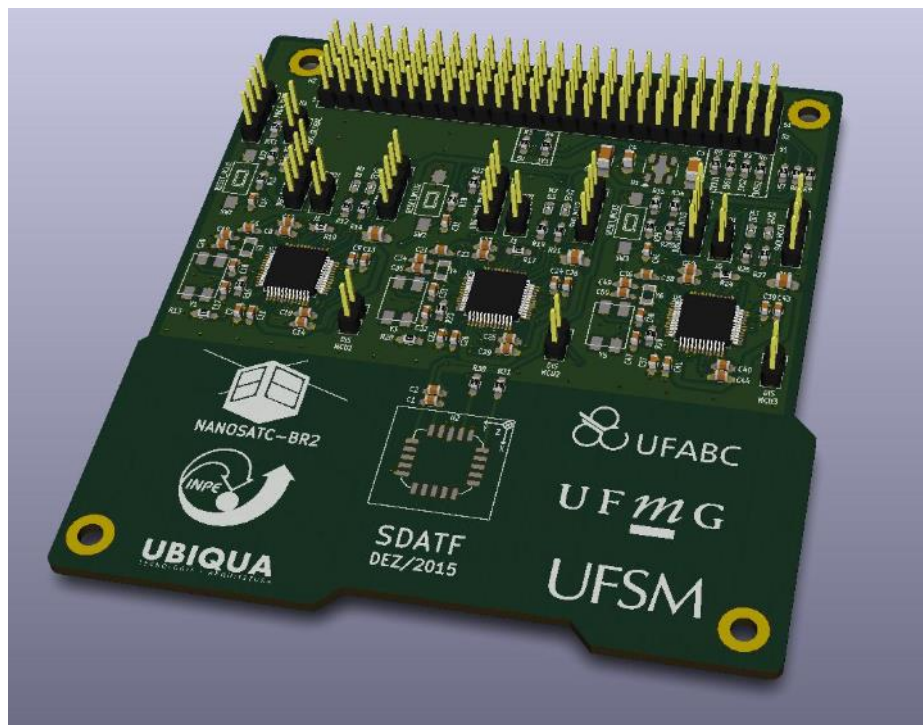


Figure 2.4 – Imagem superior do SDATF

The attitude determination is based on data from the magnetometer and data from solar sensors of the nanosatellite. Cubesats usually have six sun sensors, one for each side of the satellite. The input data of the solar sensor, the time of the measurement and the Two Line Elements will be provided by the on board computer. The attitude determination software, written in C programming language, is part of the SDATF, and it provides the attitude in terms of quaternions. This software is discussed in details in Chapter 4. Chapter 2 provides background information about the topics that will be discussed in following chapters, therefore if you do not have enough knowledge about attitude determination, I suggest you to read this chapter. Chapter 3 presents the mathematical models utilized to determine the magnetic vector and the sun position vector, and also presents other models found in literature that also

determine these vectors. Chapter 5 presents the simulation results and error analysis of the mathematical models. Chapter 4 presents the schedule of the activities performed during the development of this bachelor's dissertation. Finally, Chapter 5 presents the conclusions of the present work.

1.3 OBJECTIVES

The objectives of this bachelor's dissertation is:

- To study and simulate the attitude determination software of the NanoSatC-BR2;
- To analyze the attitude determination software of the NanoSatC-BR2 through the error analysis of the mathematical model which determines the sun position vector in the inertial frame and the mathematical model which determines the magnetic field vector in the inertial frame.

2 BACKGROUND INFORMATION

This chapter covers the following topics: coordinates systems, attitude determination, orbital elements and time measurements. If you are already familiar with these topics, you can skip this chapter.

2.1 COORDINATE SYSTEMS

In this section, coordinate systems used in the present work will be discussed.

2.1.1 GEOCENTRIC INERTIAL COORDINATE SYSTEM

The origin of this system is at the Earth's center (geocentric). The z-axis points to the vernal equinox (Y), the x-axis points to the Greenwich Meridian, the z-axis points to the North Pole and the y-axis is perpendicular to the x-axis and the z-axis. This coordinate can also be called as Geocentric Equatorial Coordinate System or Earth-Centered Inertial (ECI) system.

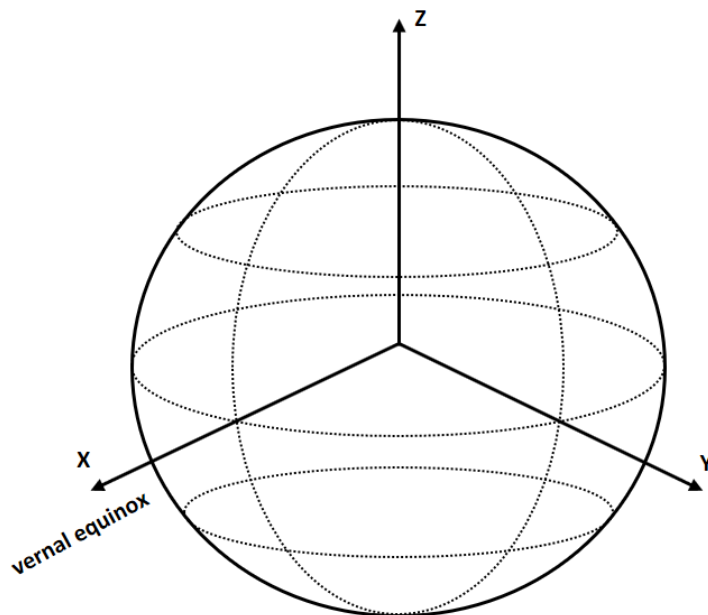


Figure 2.1 – Geocentric Inertial Coordinate System

2.1.2 TERRESTRIAL CARTESIAN COORDINATES SYSTEM

The origin of this system is at the Earth's center (geocentric). The z-axis points to the North Pole, the x-axis points to the Greenwich Meridian, the z-axis points to the North Pole and the y-axis is perpendicular to the x-axis and the z-axis. This system is rotating with Earth.

These coordinates also can be represented by angles such as terrestrial longitude (ϕ_{long}), geocentric latitude (λ_{lat}) and geocentric distance d . The relationship between Cartesian and Spherical Coordinates are shown in Figure 2.2:

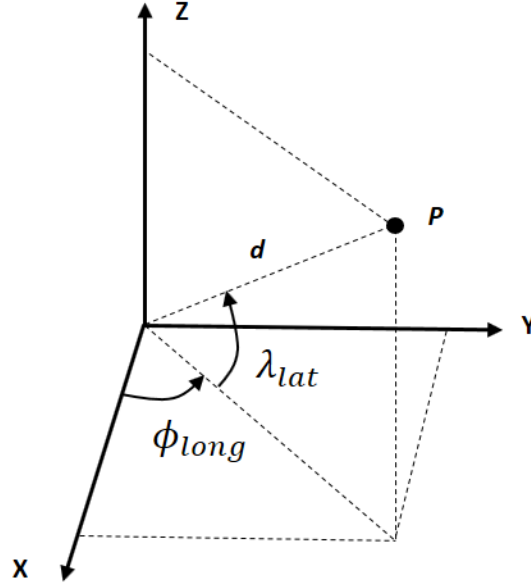


Figure 2.2 – Relation between Cartesian (x,y,z) and Spherical Coordinates ($d, \lambda_{lat}, \phi_{long}$).

Using Figure 2.2, one can write that

$$d = \sqrt{x^2 + y^2 + z^2}$$

$$\lambda_{lat} = \sin^{-1} \frac{z}{d}$$

$$\phi_{long} = \tan^{-1} \frac{y}{x}$$

Note that $-\pi \leq \phi_{long} \leq \pi$, so if you desire only positive numbers of longitude, it is necessary to add 360° to the result, and then we have the longitude ranging from 0° to 360° , that is, we have what we call “east longitude”.

2.1.3 BODY-FIXED COORDINATE SYSTEM

This coordinate system is fixed with respect to the spacecraft body, and its origin is at the center of mass of the body. The z-axis points to the nadir direction, the y-axis points in the direction to the negative orbit normal and the x-axis (same direction of the velocity vector) is perpendicular to the y-axis and the z-axis.

2.3 ATTITUDE DETERMINATION

According to Hall (2013), attitude is the orientation of a spacecraft in space, and it is determined using sensors such as sun sensors, magnetometers, star trackers, etc. It is important to know the orientation of a spacecraft because many of its equipments shall be pointed to a determined direction. For example, spacecrafts may have cameras, solar panels and communication antennas that shall be pointed to a determined direction. However, it is not only important to know the actual attitude of the spacecraft, but also to know the desired attitude in order to control the attitude throughout the use of actuators, which are systems that apply torques to achieve a desired attitude. Some examples of actuators are thrusters, spin stabilization, momentum wheels, etc. The system which encompasses both the attitude and control of a spacecraft is called Attitude Determination and Control System (ADCS).

The attitude determination is based on collecting vector components in the body frame and in the inertial reference frame from sensors and mathematical models, respectively. These vectors are utilized in algorithms in order to determine the attitude of a spacecraft, which can be represented in the form of quaternions, Euler angles or rotation matrices (Hall D., 2003). For example, the attitude matrix can be expressed as a rotation matrix (A), that is, it can be expressed as a matrix which rotates vectors from the reference frame (V) to the spacecraft frame (W):

$$A\widehat{V}_i = \widehat{W}_i \quad (2.1)$$

Where i represents the sensors. Here, $i=m$ for the vectors related to the magnetic field and $i=s$ for the vectors related to the sun position.

According to Castro (2006), methods of attitude determination can be divided into deterministic methods, such as the TRIAD method, and statistical methods, which determine the attitude throughout the minimization of the loss function. Some examples of optimum methods are the q-method and the QUEST method. This latest method was utilized in this work.

2.3.1 TRIAD

In 1964, Harold D. Black published the first method which was implemented in the attitude determination of spacecrafts using body and reference observations. The physicist Malcom Shuster later named this method as “TRIAD”, which is a name that can be considered a mention for the word triad (group of three) or can be considered an acronym for “TRlaxial Attitude Determination” (Crassidis and Markley, 2014).

Considering two measured vectors in the body frame ($\widehat{\mathbf{W}}_1$ and $\widehat{\mathbf{W}}_2$), and two known vectors in the inertial frame ($\widehat{\mathbf{V}}_1$ and $\widehat{\mathbf{V}}_2$), it is possible to determine two triads with vectors in the body (b) and inertial frame (i) (HALL, D., 2003):

$$\mathbf{t}_{1b} = \frac{\widehat{\mathbf{W}}_1}{\|\widehat{\mathbf{W}}_1\|} \quad (2.1)$$

$$\mathbf{t}_{2b} = \frac{\widehat{\mathbf{W}}_1 \times \widehat{\mathbf{W}}_2}{\|\widehat{\mathbf{W}}_1 \times \widehat{\mathbf{W}}_2\|} \quad (2.2)$$

$$\mathbf{t}_{3b} = \mathbf{t}_{1b} \times \mathbf{t}_{2b} \quad (2.3)$$

$$\mathbf{t}_{1i} = \frac{\widehat{\mathbf{V}}_1}{\|\widehat{\mathbf{V}}_1\|} \quad (2.4)$$

$$\mathbf{t}_{2i} = \frac{\widehat{\mathbf{V}}_1 \times \widehat{\mathbf{V}}_2}{\|\widehat{\mathbf{V}}_1 \times \widehat{\mathbf{V}}_2\|} \quad (2.5)$$

$$\mathbf{t}_{3i} = \mathbf{t}_{1i} \times \mathbf{t}_{2i} \quad (2.6)$$

This method assumes that vectors V or W with subscript “1” are more accurate than the vectors with subscript “2”.

Therefore, we obtain two matrices throughout the use of a triad of vectors found above:

$$\mathbf{A}_b = [\mathbf{t}_{1b} \quad \mathbf{t}_{2b} \quad \mathbf{t}_{3b}] \text{ and } \mathbf{A}_i = [\mathbf{t}_{1i} \quad \mathbf{t}_{2i} \quad \mathbf{t}_{3i}] \quad (2.7)$$

Thus, the attitude matrix can be written as:

$$\mathbf{A}_{triad} = [\mathbf{t}_{1b} \quad \mathbf{t}_{2b} \quad \mathbf{t}_{3b}][\mathbf{t}_{1i} \quad \mathbf{t}_{2i} \quad \mathbf{t}_{3i}]^T \quad (2.8)$$

2.3.2 QUATERNION

In order to understand how statistical methods work, it is first necessary to understand what is a quaternion, and its relationship with the attitude matrix of a spacecraft. A quaternion $\bar{\mathbf{q}}$ is a 4x1 vector that can be written as (Hall D., 2003):

$$\bar{\mathbf{q}} = \begin{bmatrix} q_1 \\ q_2 \\ q_3 \\ q_4 \end{bmatrix} = \begin{bmatrix} \mathbf{q} \\ q_4 \end{bmatrix} \quad (2.9)$$

Where the component \mathbf{q} is a vector, and q_4 is a scalar. These two components can be expressed as function of the Euler angles $\boldsymbol{\phi}$, and as function of the Euler axis \mathbf{n} :

$$\mathbf{q} = \mathbf{n} \sin \frac{\phi}{2} \quad (2.10)$$

$$q_4 = \cos \frac{\phi}{2} \quad (2.11)$$

Therefore, the attitude matrix can be expressed as function of quaternions:

$$\mathbf{A} = (q_4^2 - |\mathbf{q}|^2)\mathbf{I}_{3 \times 3} + \mathbf{q}\mathbf{q}^T - 2q_4[\mathbf{q}^\times] \quad (2.12)$$

Where $\mathbf{I}_{3 \times 3}$ is a 3x3 identity matrix and $[\mathbf{q}^\times]$ can be written as:

$$[\mathbf{q}^\times] = \begin{bmatrix} 0 & -q_3 & q_2 \\ q_3 & 0 & -q_1 \\ -q_2 & q_1 & 0 \end{bmatrix} \quad (2.13)$$

The attitude matrix can also be written as follows (Marques, 2000):

$$A = \begin{bmatrix} q_1^2 - q_2^2 - q_3^2 + q_4^2 & 2(q_1q_2 + q_4q_3) & 2(q_3q_1 - q_4q_2) \\ 2(q_2q_1 - q_4q_3) & -q_1^2 + q_2^2 - q_3^2 + q_4^2 & 2(q_3q_2 + q_4q_1) \\ 2(q_3q_1 + q_4q_2) & 2(q_3q_2 - q_4q_1) & -q_1^2 - q_2^2 + q_3^2 + q_4^2 \end{bmatrix} \quad (2.14)$$

2.3.3 Q-METHOD

The statistical methods can be utilized if there are more than two observations available and none information is going to be disregarded.

The Wahba's problem, posed by Grace Wahba in 1965, is a way of finding the attitude matrix that minimizes the following equation, most known as *loss function*:

$$\begin{aligned} L(A) &= \frac{1}{2} \sum_{i=1}^n a_i (\widehat{\mathbf{W}}_i - A\widehat{\mathbf{V}}_i)^2 \\ &= \frac{1}{2} \sum_{i=1}^n a_i (\widehat{\mathbf{W}}_i^T \widehat{\mathbf{W}}_i + \widehat{\mathbf{V}}_i^T \widehat{\mathbf{V}}_i - 2\widehat{\mathbf{W}}_i^T A\widehat{\mathbf{V}}_i) \end{aligned} \quad (2.15)$$

Where n is the number of observations and a_i is the weight related to each vector i .

The vector is normalized to unity, that is, $\widehat{\mathbf{W}}_i^T \widehat{\mathbf{W}}_i = \widehat{\mathbf{V}}_i^T \widehat{\mathbf{V}}_i = 1$. Therefore, the loss function can be written as:

$$L(A) = \sum_{i=1}^n a_i (1 - \widehat{\mathbf{W}}_i^T A \widehat{\mathbf{V}}_i) \quad (2.16)$$

This method aims to maximize the following gain function (and consequently, minimizes the loss function):

$$g(A) = 1 - L(A) \quad (2.17)$$

Substituting Equation 2.16 into Equation 2.17, and noting that $\sum_{i=1}^n a_i = 1$:

$$g(A) = \sum_{i=1}^n a_i (\widehat{\mathbf{W}}_i^T A \widehat{\mathbf{V}}_i) \quad (2.18)$$

Where $\widehat{\mathbf{V}}_i$ are the reference vectors, $\widehat{\mathbf{W}}_i$ are the observation vectors, and n are the number of sensors installed on the spacecraft (Duarte et al, 2009).

The gain function can also be written in terms of quaternions:

$$g(A) = (q_4^2 - \mathbf{q} \cdot \mathbf{q}) \text{tr} B^T + 2 \text{tr} [\mathbf{q} \mathbf{q}^T \mathbf{B}^T] - 2 q_4 \text{tr} [\mathbf{q}^\times \mathbf{B}^T] \quad (2.19)$$

$$\text{or } g(\bar{\mathbf{q}}) = \bar{\mathbf{q}}^T \mathbf{K} \bar{\mathbf{q}} \quad (2.20)$$

Where \mathbf{K} can be expressed as:

$$\mathbf{K} = \begin{bmatrix} \mathbf{S} - \sigma \mathbf{I} & \mathbf{Z} \\ \mathbf{Z}^T & \sigma \end{bmatrix} \quad (2.21)$$

And B, σ, S e Z can be written, respectively, as the following:

$$\mathbf{B} = \sum_{i=1}^n a_i (\widehat{\mathbf{W}}_i \widehat{\mathbf{V}}_i^T) \quad (2.22)$$

$$\sigma = \text{tr} \mathbf{B} = \sum_{i=1}^n a_i \widehat{\mathbf{W}}_i^T \widehat{\mathbf{V}}_i \quad (2.23)$$

$$\mathbf{S} = \mathbf{B} + \mathbf{B}^T = \sum_{i=1}^n a_i (\widehat{\mathbf{W}}_i \widehat{\mathbf{V}}_i^T + \widehat{\mathbf{V}}_i \widehat{\mathbf{W}}_i^T) \quad (2.24)$$

$$\mathbf{Z} = \sum_{i=1}^n a_i (\widehat{\mathbf{W}}_i \times \widehat{\mathbf{V}}_i) = [B_{23} - B_{32} \quad B_{31} - B_{13} \quad B_{12} - B_{21}]^T \quad (2.25)$$

In order to determine the attitude, it is necessary to maximize the equation 2.19 by taking the first derivative of it with respect to $\bar{\mathbf{q}}$:

$$g'(\bar{\mathbf{q}}) = \bar{\mathbf{q}}^T \mathbf{K} \bar{\mathbf{q}} - \lambda \bar{\mathbf{q}}^T \bar{\mathbf{q}} \quad (2.26)$$

The equation above is stationary when:

$$K\bar{q}_{opt} = \lambda\bar{q}_{opt} \quad (2.27)$$

λ can be calculated as an eigenvalue of K and \bar{q}_{opt} as the eigenvector of K . The attitude corresponds to the maximum value of λ and its eigenvector \bar{q}_{opt} , that is, the optimum quaternion provides the estimated attitude (Duarte et al, 2009).

2.3.4 QUEST (QUaternion ESTimator)

The QUEST method was proposed by Shuster and Oh (1981), and it also has the aim to minimize the loss function (Duarte et al, 2009):

$$L(A) = \frac{1}{2} \sum_{i=1}^n a_i (\widehat{\mathbf{W}}_i - A\widehat{\mathbf{V}}_i)^2 \quad (2.28)$$

And maximize the gain function:

$$g(\bar{q}) = \sum_{i=1}^n a_i \widehat{\mathbf{W}}_i^T A \widehat{\mathbf{V}}_i = \lambda_{opt} \quad (2.29)$$

Where A is the attitude matrix, $\widehat{\mathbf{W}}_i$ is the vector measured in the body frame of the spacecraft and $\widehat{\mathbf{V}}_i$ is the vector in the inertial frame.

The solution for an optimum value of the eigenvalue λ is given by the following equation after rearranging equations 2.28 and 2.29:

$$\lambda_{opt} \approx \sum_{i=1}^n a_i - L(A) \quad (2.30)$$

Evidentially, to find an optimum value, we need a small loss function. Therefore, λ_{opt} can be approximated as:

$$\lambda_{opt} \approx \sum_{i=1}^n a_i \quad (2.31)$$

After estimating the optimum eigenvalue, the correspondent eigenvector (quaternion) which corresponds to the optimal attitude estimate can be determined (Hall, D., 2003).

Converting the quaternion to Rodrigues Parameters (\mathbf{p}):

$$\mathbf{p} = \frac{\bar{q}}{q_4} = \hat{X} \tan \frac{\theta}{2} \quad (2.32)$$

Where \hat{X} is the axis rotation and θ is the angle rotation about \hat{X} .

Therefore,

$$\mathbf{p} = [(\lambda_{opt} + \sigma)\mathbf{I} - \mathbf{S}]^{-1}\mathbf{Z} \quad (2.33)$$

After determining the Rodrigues parameters, it is possible to determine the quaternion by the following way:

$$\bar{q} = \frac{1}{\sqrt{1 + \mathbf{p}^T \mathbf{p}}} \begin{bmatrix} \mathbf{p} \\ 1 \end{bmatrix} \quad (2.34)$$

However, when the angle rotation is π , \mathbf{p} is infinite. For implementation purposes, when $\sqrt{1 + \mathbf{p}^T \mathbf{p}} = 0$, or $\mathbf{p}^T \mathbf{p} = -1$, we set the quaternion to $[0 \ 0 \ 0 \ 1]^T$. For more details, see references Shuster (1978) and Shuster and Oh (1981).

2.4 ORBITAL ELEMENTS

This section will present the orbital elements of a body orbiting another body, such as the semi-major axis, semi-minor axis, eccentricity, inclination, etc.

a) Semi-Major Axis (a) and Minor Semi-Axis (b)

The semi-major axis a is the distance from the center of ellipse to its apogee or perigee (Figure 2.1); thus, the distance from the apogee to the perigee along the horizontal axis (major axis) is $2a$. On the other hand, b is one half of the vertical axis (minor axis).

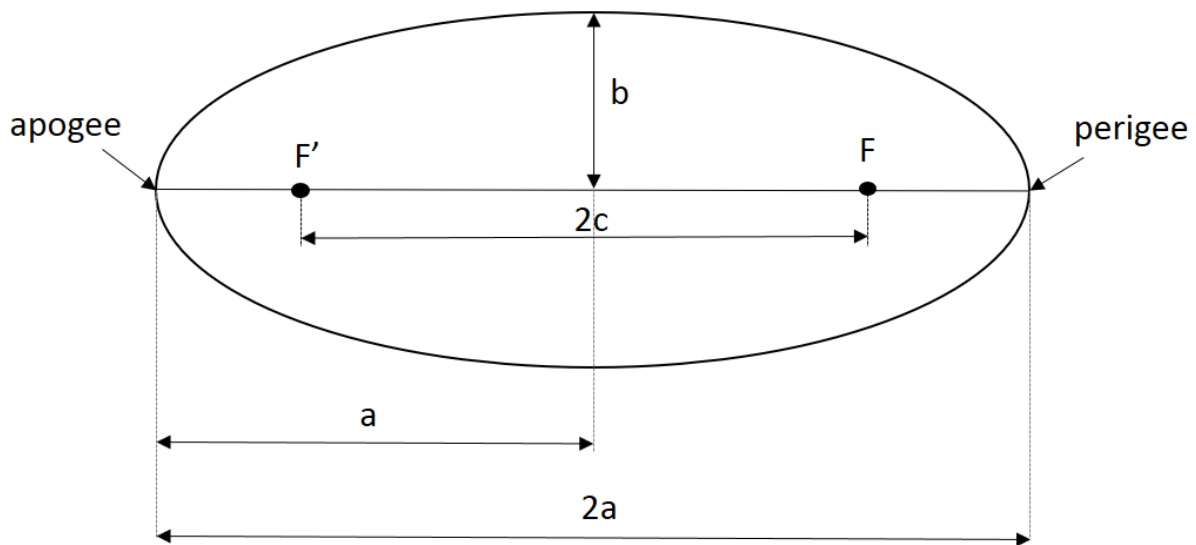


Figure 2.1 – Semi-major axis (a) and semi minor axis (b) and distance between two foci ($2c$)

In addition, the distance between the two foci is $2c$, and the semi-minor axis b is related to the semi-major axis as follows:

$$b = a(1 - e^2)^{1/2} \quad (2.35)$$

Note that for a body orbiting Earth, “perigee” and “apogee” are the names given to the nearest and farthest point of the body’s orbit around the Earth, respectively. For bodies orbiting the Sun, “perihelion” and “aphelion” are the names given to the nearest and farthest points of a body’s orbit around the Sun.

b) Eccentricity (e)

Eccentricity determines the shape of an orbit. For example,

- $e = 0$, for a circular orbit;
- $0 < e < 1$, for an elliptical orbit;
- $e = 1$, for a parabolic trajectory;
- $e > 1$, for a hyperbolic trajectory.

Eccentricity can be related to the major axis and the distance between two foci as the follows (Sellers, 2004):

$$e = \frac{2c}{2a} \quad (2.36)$$

It is important to note that the eccentricities of the orbits of the planets change with time due to planetary perturbations.

c) Inclination (i)

Inclination (i) is basically the angle between the equatorial plane and the orbital plane (Figure 2.2). More specifically, it can be determined as the angle between \hat{K} , vector that points to the North Pole of Earth, and \vec{h} (the specific angular momentum vector). The specific angular momentum vector can be expressed as (Figure 2.2):

$$\vec{h} = \vec{R} \times \vec{V} \quad (2.37)$$

Where \vec{R} is the position vector of the satellite (km) and \vec{V} is the velocity of the spacecraft.

Note that this case is considering a satellite orbiting Earth, but it can be utilized for other bodies orbiting Earth or orbiting other kind of objects.

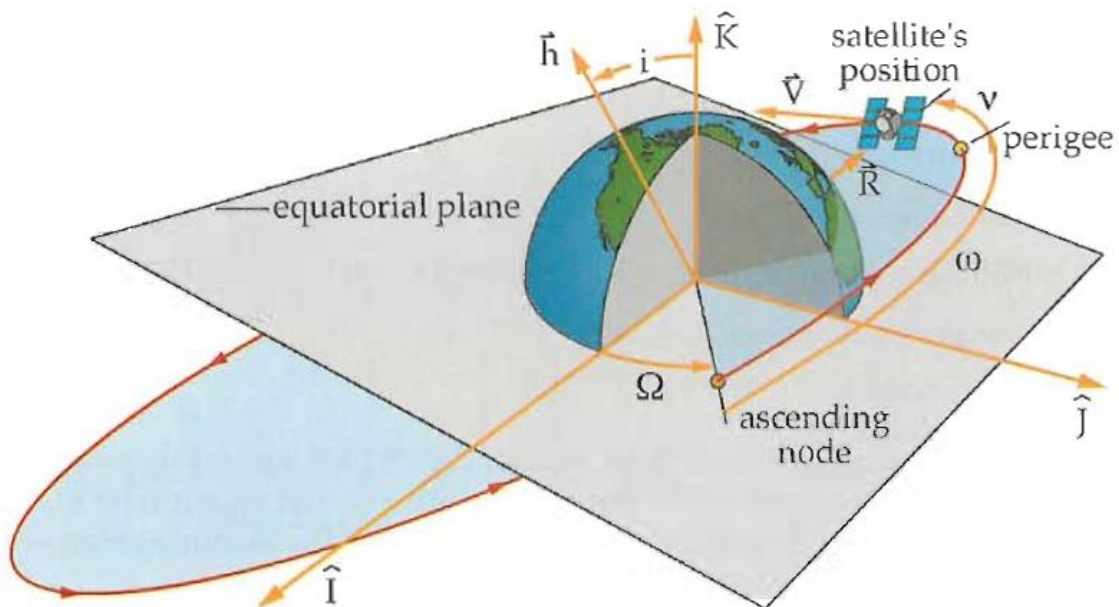


Figure 2.2 – Orbital Elements: inclination (i), Right Ascension of the Ascending Node (Ω), Argument of Perigee (w) and True Anomaly (v). Source: Sellers (2004)

Inclination is used to define different kinds of orbits. For example,

- $i = 0^\circ$ or $i = 180^\circ$, for an equatorial orbit;
- $i = 90^\circ$, for polar orbit;

Inclination can also be divided into two major classes in relation to the direction that the spacecraft or satellite is moving:

- Direct Orbit or Prograde Orbit ($0^\circ \leq i < 90^\circ$): the spacecraft/satellite is moving in the same direct of the Earth's rotation;
- Indirect Orbit or Retrograde Orbit ($90^\circ < i \leq 180^\circ$): the spacecraft/satellite is moving in the opposite direction of the Earth's rotation.

d) Right Ascension of the Ascending Node – RAAN (Ω)

The right ascension of the ascending node is the angle between principal direction \hat{l} , which is a vector that points to the direction of the vernal equinox, and the ascending node (Figure 2.2). The ascending node is the point where the orbital plane intersects the equatorial plane when the spacecraft is heading north, that is, when the spacecraft is going from south to north. The range of this orbital element is from 0° to 360° .

For geocentric orbits, we usually use the name RAAN for this angle, however, when we are considering planets orbiting the sun, we usually call this angle as Longitude of the Ascending Node (N).

e) Argument of Perigee (w)

The argument of the perigee is the angle between the ascending node and the perigee (Figure 2.2). Note that the angle between the ascending node and the perihelion is called Argument of the Perihelion. This orbital element ranges from 0° to 360° .

f) True Anomaly (v)

True Anomaly is the angle between the perigee and the position vector of the spacecraft (\vec{R}), and it ranges from 0° to 360° . This is the only orbital element described until now that changes with time (Sellers, 2004).

2.4.1 OTHER ORBITAL ELEMENTS

In this section, other orbital elements which are necessary to calculate the sun position vector will be presented. In addition, some orbital elements presented in Section 2.4 will be re-written in function of other elements.

The Sun (S) seems to execute an apparent and counterclockwise orbit around the Earth (G) from a geocentric point of view as it is depicted in Figure 2.3 (Fitzpatrick, 2010). The sun traces out a circle on the celestial sphere that is called *ecliptic* circle. This circle is inclined at 23.44° to the *celestial equator*, which is the projection of the equator of Earth on the celestial sphere (Defense Dept. Naval Observatory, 2014). This inclination is commonly known as Obliquity of the Ecliptic (ϵ), and it decreases with time due to planetary perturbations. In addition, the symbols A and Π , in Figure 2.3, represent the apogee and perigee of the ellipse, respectively.

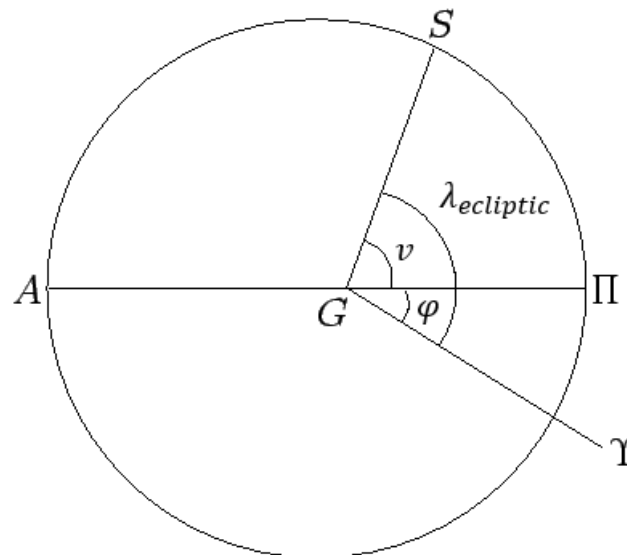


Figure 2.3 – Apparent orbit of the Sun around our planet. Source: Fitzpatrick (2010)

For an apparent orbit of the Sun, the point where the ecliptic intersects the celestial equator from south to north is called Vernal Equinox (Υ), because the Longitude of the Ascending Node is zero in this case. The angle between the Vernal Equinox and the Sun's perigee (Π) is called Longitude of the Perigee (φ). The Ecliptic Longitude ($\lambda_{ecliptic}$) of the Sun is the angle between the Vernal Equinox and the Sun position, as it can be seen in Figure 2.3. As explained before, true anomaly (v) is the position of the orbiting body measured from the perigee, so in this case, v is the angle between perigee and the Sun. Consequently, it is

possible to write that the ecliptic longitude ($\lambda_{ecliptic}$) is the sum of the longitude of the perigee and the true anomaly:

$$\lambda_{ecliptic} = \varphi + v \quad (2.38)$$

Ecliptic Latitude ($\beta_{ecliptic}$) is the angle between the ecliptic and the object towards the north ecliptic pole or south ecliptic pole. For the sun, this angle is approximated zero.

Mean Anomaly (M) is the angle between the apogee and the Sun if this star were moving in a circular orbit instead of the elliptical orbit, but with a constant angular velocity and with the same orbital period of the Sun moving in the elliptical orbit. By analogy, it is possible to write that the Mean Longitude is the sum of the Longitude of the Perigee and the Mean Anomaly:

$$\lambda_M = \varphi + M \quad (2.39)$$

The Eccentric Anomaly (E) is the angle between the perigee and the projection of the Sun into the circular orbit (Wertz, 2002), as seem is Figure 2.4.

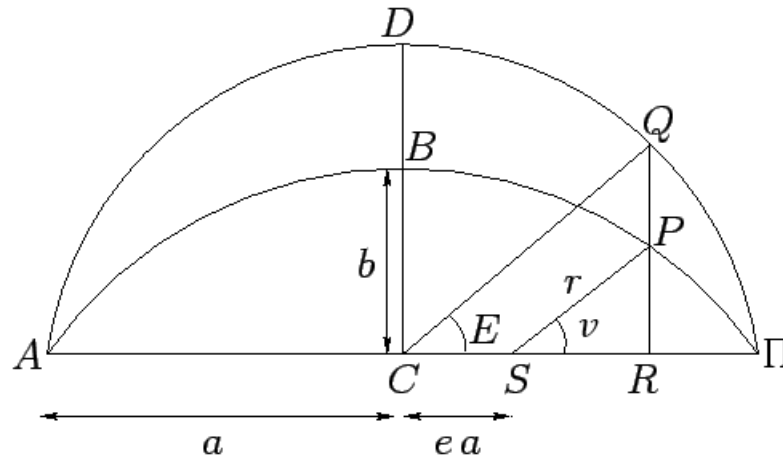


Figure 2.4 – Half elliptical and circular orbit. Source: Fitzpatrick (2010)

In the figure above, A represents the aphelion, Π represents the perihelion, S represents the focus in which the Sun is located, P represents a planet orbiting the Sun, C represents the geometric center of the orbit, v represents the true anomaly, e represents the eccentricity, r

represents the radial distance between the sun and the planet, a represents the semi-major axis and b represents the semi-minor axis.

Fitzpatrick (2010) demonstrates the relationship between M and E as follows.

The equation of the ellipse ΠPBA of the Figure 2.4, is given as:

$$\frac{x^2}{a^2} + \frac{y^2}{b^2} = 1 \quad (2.40)$$

The equation of the circle ΠQDA is given as:

$$\frac{x'^2}{a^2} + \frac{y'^2}{a^2} = 1 \quad (2.41)$$

If $x' = x$, then:

$$\frac{y}{y'} = \frac{b}{a} = \frac{RP}{RQ} \quad (2.42)$$

According to Equation 2.36, $CS = ea$. Using trigonometry identities, it is easy to verify that $SR = r \cos v$, $RP = r \sin v$, $CR = a \cos E$ and $RP = r \sin E$. Consequently, Equation 2.42 can be written as follows:

$$r \sin v = b \sin E \quad (2.43)$$

Substituting Equation 2.35 into Equation 2.43:

$$r \sin v = b \sin E = a(1 - e^2)^{1/2} \sin E \quad (2.44)$$

According to Figure 2.4, $SR = CR - CS$. Consequently,

$$r \cos v = a(\cos E - e) \quad (2.45)$$

Squaring the Equations 2.44 and 2.45, and then summing them gives the next equation:

$$r = a(1 - e \cos E) \quad (2.46)$$

Combining the latest equation to Equation 2.45:

$$\cos v = \frac{\cos E - e}{1 - e \cos E} \quad (2.47)$$

According to Kepler's second law, a line linking planets of our solar system and the Sun sweeps out equal areas during equal intervals of time. Therefore,

$$\frac{\text{Area} \Pi PS}{\pi ab} = \frac{t - t^*}{\tau} \quad (2.48)$$

Where t^* is the time of the planet at the perihelion, t is the time at P and τ is the orbital period.

The area ΠPS can also be written as

$$\text{Area} \Pi PS = \text{Area} SRP + \text{Area} \Pi RP = \frac{1}{2} r^2 \cos v \sin v + \text{Area} \Pi RP \quad (2.49)$$

However, $\frac{RQ}{RP} = \frac{b}{a}$ is valid for all values of v . Therefore,

$$\text{Area} \Pi PS = \frac{b}{a} \text{Area} \Pi RQ \quad (2.50)$$

In addition,

$$\text{Area} \Pi RQ = \text{Area} \Pi QC - \text{Area} RQC = \frac{1}{2} E a^2 - \frac{1}{2} a^2 \cos E \sin E \quad (2.51)$$

Therefore, substituting Equations 2.50 and 2.51 into Equation 2.49:

$$\frac{t - t^*}{\tau} \pi ab = \frac{1}{2} r^2 \cos v \sin v + \frac{b a^2}{a} (E - \cos E \sin E) \quad (2.52)$$

Substituting Equations 2.44 and 2.45 into Equation 2.52, and using trigonometry identities, we have the following equation, commonly known as the Kepler's Equation:

$$M = E - e \sin E \quad (2.53)$$

Where $M = \left(\frac{2\pi}{\tau}\right) (t - t_*)$.

In summary, all these calculations led to three equations that were all in function of E . These equations are the Equation 2.45, 2.46 and 2.53. For small eccentricities ($e \ll 1$), these three equations can be expanded to give the following equations:

$$E = M + e \sin M + \frac{1}{2} e^2 \sin 2M \quad (2.54)$$

$$r = a(1 - e \cos v - e^2 \sin^2 v) \quad (2.55)$$

$$v = E + e \sin E + \frac{1}{4} e^2 \sin 2E \quad (2.56)$$

Combining the equations above, it is possible to write v as a function of M :

$$v = M + 2e \sin M + \left(\frac{5}{4}\right) e^2 \sin 2M \quad (2.57)$$

Now it is easy to write the Ecliptic Longitude in function of the Mean Longitude and the Mean Anomaly by first substituting the Equation 2.38 into Equation 2.39, and then substituting Equation 2.57 into the result of the latest substitution:

$$\lambda_{ecliptic} = \lambda_M + 2e \sin M + \left(\frac{5}{4}\right) e^2 \sin 2M \quad (2.58)$$

2.5 TIME MEASUREMENTS

Since the ancient times, the humans track time through the use of calendars. Until today a large number of calendars was developed, and the most known of them are the following: Roman calendar, Julian calendar and Gregorian calendar. The Roman calendar, and its variations, were utilized during the Roman Empire. This calendar was reformed by Julius Caesar in 46 B.C., and the new calendar was named Julian Calendar. The Julian year has 365.25 days and the Julian century has 36,525 days. In 1582, Pope Gregory XIII replaced this calendar by the Gregorian Calendar, which is the calendar currently in use.

Time is utilized to “define with precision the moment of a phenomenon”, and this moment is commonly known as the “epoch” of an event (Vallado, 1997). That is, “epoch” is the instant in which a phenomenon occurred. Nowadays, there are several time systems used to measure time, and herein, some of these systems will be presented. Before presenting the time systems, it is necessary to understand what is a Solar Day. Solar day is the “interval between successive transits of the Sun over a local meridian”, however, this interval is not uniform because the Earth’s orbit is not circular, and because the axis of the Earth’s rotation is not perpendicular to the plane of the ecliptic due to the obliquity of the ecliptic (Seago, 2016). In order to solve the problem of a non-uniform motion, the Mean Solar Day was proposed with the aim to provide days with the same hours and minutes, that is, a day with duration of 24 hours. Mean Solar Day is based on a fictitious Sun that exhibits a motion along the equator. (Vallado, 1997).

Universal time (UT) is the time system that utilizes the Mean Solar Day as the fundamental unit (Wertz, 2002), that is, UT is the Mean Solar Day counted from midnight on the Greenwich Meridian (Carvalho, 2008). There are several variations of the UT time system: UT0, UT1, UT2. UT0 is the UT time determined for a particular ground station, but UT0 is not corrected for the wander of the geographic poles, and consequently the UT0 time is different when determined in different ground stations. UT1 is the correction of UT0 due to this polar motion, and it is based on the actual angular rotation of the Earth. However, this angular motion is subject to seasonal variations, so the UT2 corrects these seasonal variations in the angular rotation of the Earth (Vallado, 1997; Wertz, 2002).

According to the National Institute of Standards and Technology (NIST), the International Atomic Time (TAI) is “computed by taking the weighted average of more than 300 atomic clocks”, located in 60 laboratories all over the world (National Institute of Standards and Technology, n.d.). An atomic clock is based on the change of the energy state

of an atom of Cesium-133. This change of energy state occurs at a known countable frequency, which is 9,192,631,770 cycles per second (Bureau International des Poids et Mesures, 2014).

Coordinated Universal Time (UTC) is a time standard based on TAI, and it was first introduced in 1972 in order to relates with UT1, which is a time standard based on the Earth's rotation. The difference between UTC and UT1 is always within $\pm 0.9s$. The leap seconds is adjusted every year by the U.S. Naval Observatory due to the variations of the Earth's rotation. The difference between UTC and TAI is always an integer number of seconds.

Terrestrial Time (TT) or Terrestrial Dynamical Time (TDT) is the “theoretical timescale of apparent geocentric ephemerides of bodies in the solar system”, in relation to the Earth's center (Wertz, 1997), and its fundamental unit is seconds. This time standard relates to the TAI time standard as follows:

$$TDT = TAI + 32.184 s \quad (2.59)$$

Barycenter Dynamic Time (TDB) is the “independent variable of equations of motion with respect to the barycenter of the solar system”. Therefore, TDB differs from TT because the latest is referred to the Earth's center and TDB is referred to the barycenter of the solar system. The TDB can be calculated according the following equation, in seconds (Schlyter, 2010):

$$TDB = TT + 0.001658 \sin 2g + 0.000014 \sin 2g \quad (2.60)$$

Where g is the mean anomaly of Earth orbiting the Sun given in degrees:

$$g = 357.53^\circ + 0.9856003^\circ(JD - 2451545.0) \quad (2.61)$$

JD is the Julian Date, which is a concept that will be explained in the next section.

2.5.1 TYPES OF JULIAN DATES

The use of calendars is not useful for computations, therefore, a new concept commonly utilized in astrodynamics was proposed by the French scholar Joseph Scaliger in 1582. This new concept is the Julian Date (JD) or Julian Day, which is the continuous amount of time measured in days from the epoch January 1, 4713 B.C. (12:00 UT - noon). According to Wertz

(2002), this new concept is named “Julian Date” because of Scaliger’s father, Julius Ceaser Scaliger, and not because of the Roman politician Julius Caesar.

The Julian Date is computed as follows (Vallado, 1997):

$$JD = 365(yr) - INT \left\{ \frac{7 \left\{ yr + INT \left(\frac{mo + 9}{12} \right) \right\}}{4} \right\} + INT \left(\frac{275mo}{9} \right) + d + 1,721,013.5$$

$$+ \frac{\left(\frac{s}{60} + min \right)}{60} + \frac{h}{24} \quad (2.62)$$

Where:

yr = year from 1900 to 2100;

mo = month from 1 to 12;

d = day from 1 to 31;

min = minutes from 0 to 59;

s = seconds from 0 to 59.999.

It is important to point out that the equation above is valid from a period from March 1, 1900 to February 18, 2100.

There are other types of Julian Dates which are utilized according to the need of the user. For example, the Julian Date for Space (JDS) is used in NASA orbit programs, and it is measured in seconds, not in days as the JD. The epoch of this concept is also different because it measures the amount of time in seconds from the epoch September 17, 1957 (0 hours UT), which is “the first Julian day divisible by 100 prior the launch of the first manmade satellite the Soviet Union on October 4, 1957” (Wertz, 2002), that is, prior the launch of the first artificial satellite Sputnik 1. JDS relates to JD as follows:

$$JDS = JD - 2,436,099.5 \quad (2.63)$$

The European Space Operation Center, a mission control centre of the European Space Agency (ESA) uses the Modified Julian Date (MJD), which is the continuous amount of time measured in days from the epoch January 1, 1950 (0 hours UT).

The software of the NanosatC-BR2 uses the MJD to perform its calculations, but it considers that the epoch starts in January 1, 1950 at midnight UT (end of the day). The MJD as per the software of the NANOSAT-BR2 developed by Dr. Valmir Carraca e Dr. Helio Kuta of INPE:

$$MJD = 367(yr) + d - 712269 + INT(floor)\left(\frac{276(m)}{9}\right) - INT(floor)\left(7\left(YR + \frac{INT(floor)\left(\frac{m+9}{12}\right)}{4}\right)\right) \quad (2.64)$$

The equation above is valid from the year 1900 to 2100. For example, the MJD for 1st January, 1950 is 0, and the MJD for 1st January, 1951 is 365.

Note that the function “floor” returns the largest integer that is smaller or equal to the value in question.

2.5.2 GREENWICH MEAN SIDERAL TIME

Greenwich Mean Sidereal Time (*GMST*) is the angle hours of the average vernal equinox relative to the meridian of Greenwich.

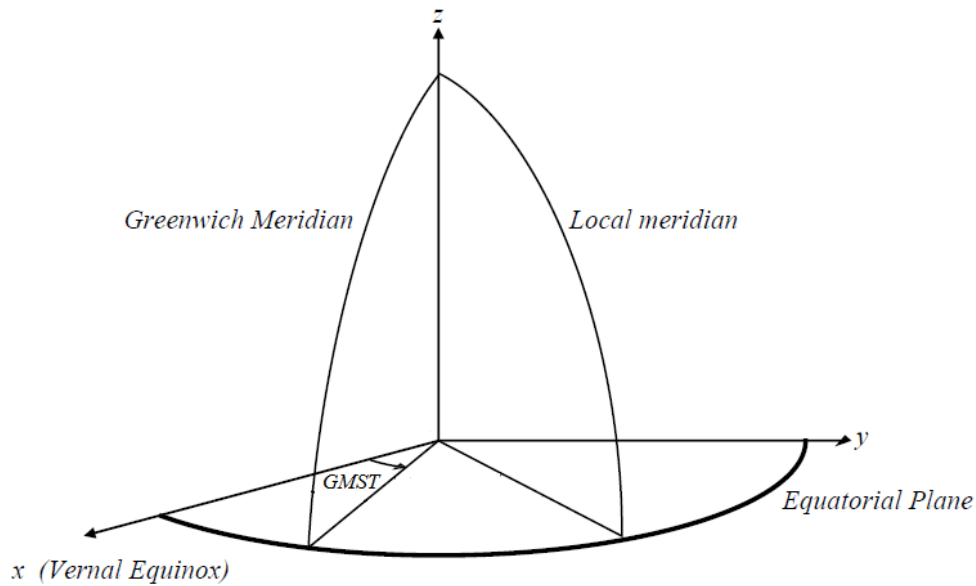


Figure 2.5 – Greenwich Mean Sidereal Time. Adapted from Murad et al. (1995)

The number of Julian Centuries (*T*) since 1st January, 2000 (UT1) is determined as follows:

$$T = \frac{MJD - 18262.5}{36525}$$

Where MJD is the Modified Julian Date.

The GMST in seconds at 0 hours (UT1) is given as (Vallado, 1997):

$$GMST_{0,sec} = 24110.54841 + (8640184.812866 + 9.3104 * 10^{-2} * T - 6.2 * 10^{-6} * T^2) * T$$

There are 86,400 seconds in one full rotation (2π), therefore the $GMST_{0,rad}$ can be written in radians as follows:

$$GMST_{0,rad} = GMST_{0,sec} * \frac{2\pi}{86,400} = GMST_{0,sec} * \frac{\pi}{42,200}$$

Finally, the radians related to the fraction of the day in seconds (fd) shall be added to the Greenwich Mean Sideral Time:

$$GMST = GMST_{0,rad} + fd * \omega_{earth}$$

Where $\omega_{earth} (\approx 7.29 * 10^{-5} \frac{rad}{s})$ is the angular speed of the Earth.

The result of GMST is divided by 2π , and the remainder is the actual GMST. If GMST less than zero, than $GMST = GMST + 2\pi$.

3 MATHEMATICAL MODELING

This chapter will present the mathematical models utilized to determine the sun position vector and the magnetic field vector of the attitude determination system on board of the NanosatC-BR2. These chapter will also present other models utilized to determine the sun position vector, such as the David Vallado`s (1997) Model and the Astronomical Almanac model (Defense Dept. Naval Observatory, 2014), because a comparison between the model of the NanosatC-BR2 and these models found in literature will be performed in Chapter 5

3.1 SUN POSITION VECTOR

There are several models to determine the sun position vector, and in the present work, the model utilized in the attitude determination system on board of the NanosatC-Br2 will be compared to others models.

3.1.1 NANOSATC-BR2 MODEL

This model has two inputs: The Modified Julian Day (mjd) and the Fraction of the day (fd) in seconds. The Modified Julian Day (MJD) starts in January 1, 1950 at midnight (Universal Time -UT1). The fraction of the day is given in seconds (fd). This model is valid from January, 1, 2000 until 2050. Therefore, this model uses the day number from January, 1, 2000, 0.0 UT (d):

$$d = MJD - 18261 \quad (3.1)$$

Where 18261 is the Modified Julian Day in December, 31, 1999 at 0:00 UT. Adding the fraction of seconds into the result of the above equation:

$$T = d + \frac{fd}{86,400} \quad (3.2)$$

Where 86,400 is the quantity of seconds per day. It is easy to verify that T is equal to zero in December, 31, 1999 at 0:00 UT.

The orbital elements of the Sun are determined as follows (Schlyter, n.d.):

$$w = 282.9404^\circ + 4.70935E - 5 T \quad (3.3)$$

$$M = 356.0470^\circ + 0.9856002585 T \quad (3.4)$$

$$e = 0.016709 - 1.151E - 9 T \quad (3.5)$$

Where w is the argument of perihelion, M is the mean anomaly and e is the eccentricity.

The ecliptic longitude ($\lambda_{ecliptic}$) is the sum of the longitude of the perigee (φ) and the true anomaly (v):

$$\lambda_{ecliptic} = \varphi + v \quad (3.6)$$

The longitude of the perigee is given as:

$$\varphi = N + w \quad (3.7)$$

Where N is the longitude of the ascending node, which is equal to zero for the Sun. Therefore,

$$\lambda_{ecliptic} = w + v \quad (3.8)$$

The sun longitude can be approximated as the sum of the true anomaly and the argument of perihelion:

$$\lambda_{ecliptic} = M + 2e \sin M + 1.25e^2 \cos M + w \quad (3.9)$$

The true anomaly is given as (Chauhan, 2008):

$$v = M + \left(2e - \frac{1}{4}e^3\right) \sin M + \frac{5}{4}e^2 \sin 2M + \frac{13}{12}e^3 \sin 3M \quad (3.10)$$

Neglecting the third power of e :

$$v = M + 2e \sin M + \frac{5}{4}e^2 \sin 2M \quad (3.11)$$

As $\sin 2M \approx 2 \cos M \sin M$,

$$v = M + 2e \sin M + 2.5 e^2 \cos M \sin M \quad (3.12)$$

Therefore, the ecliptic longitude is

$$\lambda_{ecliptic} = w + M + 2e \sin M + 2.5 e^2 \cos M \sin M \quad (3.13)$$

The obliquity of the ecliptic is given as follows,

$$\epsilon = 23.4394^\circ - 3.563E - 7 * T [deg] \quad (3.14)$$

Therefore, the sun position vector in equatorial, rectangular geocentric coordinates is given as follows:

$$x = r \cos \lambda_{ecliptic} \quad (3.15)$$

$$y = r \sin \lambda_{ecliptic} \cos \epsilon \quad (3.16)$$

$$z = r \sin \lambda_{ecliptic} \sin \epsilon \quad (3.17)$$

This model considers the distance from Earth to Sun (r) equal to 1 Astronomical Unit. Thus, the final coordinates can be written as:

$$x = \cos \lambda_{ecliptic} \quad (3.18)$$

$$y = \sin \lambda_{ecliptic} \cos \epsilon \quad (3.19)$$

$$z = \sin \lambda_{ecliptic} \sin \epsilon \quad (3.20)$$

The coordinates above are given in Astronomical Units.

3.1.2 DAVID VALLADO'S MODEL

The following model is presented in (Vallado, 1997). This is a 0.01° accuracy model, and it is valid from 1950 to 2050. The input of this model is the Julian Date (JD), which is the continuous amount of time measured in days from the epoch January 1, 4713 B.C. (12:00 UT). However, the model uses the Julian Date (JD) which measures the continuous count of days since 0:00 UT on January 1, 4713 B.C.

First, the number of Julian centuries T_{UT1} from the epoch J2000 is found using the following equation:

$$T_{UT1} = \frac{JD_{UT1} - 2,451,545.0}{36,525} \quad (3.21)$$

The mean longitude of the Sun is computed as follows:

$$\lambda_M = 280.4606184^\circ + 36,000.77005361 T_{UT1} \quad (3.22)$$

It is possible to calculate the mean anomaly for the Sun through the following equation:

$$M = 257.5277233^\circ + 35,999.05034 T_{TDB} \quad (3.23)$$

This models assumes that $T_{TDB} \approx T_{UT1}$. TBD stands for Barycentric Dynamical Time.

The true anomaly is written as follows:

$$v = M + 2e \sin M + \frac{5}{4}e^2 \sin 2M \quad (3.24)$$

Where the eccentricity of Earth's orbit is $e = 0.0016708617$.

The ecliptic longitude and the ecliptic latitude are given as follows:

$$\lambda_{ecliptic} = \lambda_M + 1.914666471^\circ \sin M + 0.01994643 \sin 2M \quad (3.25)$$

$$\beta_{ecliptic} = 0^\circ \quad (3.26)$$

The obliquity of ecliptic is given as:

$$\epsilon = 23.439291^\circ - 0.013004 T_{TBD} \quad (3.27)$$

Again, it is possible to considers that $T_{TDB} \approx T_{UT1}$.

The magnitude of the distance to the Sun is,

$$r = 1.00140612 - 0.016708617 \cos M - 0.000139589 \cos 2M \quad (3.26)$$

Finally, the position vector (Figure 3.1) in geocentric equatorial coordinates (ECI) is

$$x = r \cos \lambda_{ecliptic} \quad (3.27)$$

$$y = r \cos \epsilon \sin \lambda_{ecliptic} \quad (3.28)$$

$$z = r \sin \epsilon \sin \lambda_{ecliptic} \quad (3.29)$$

The coordinates above are given in Astronomical Units.

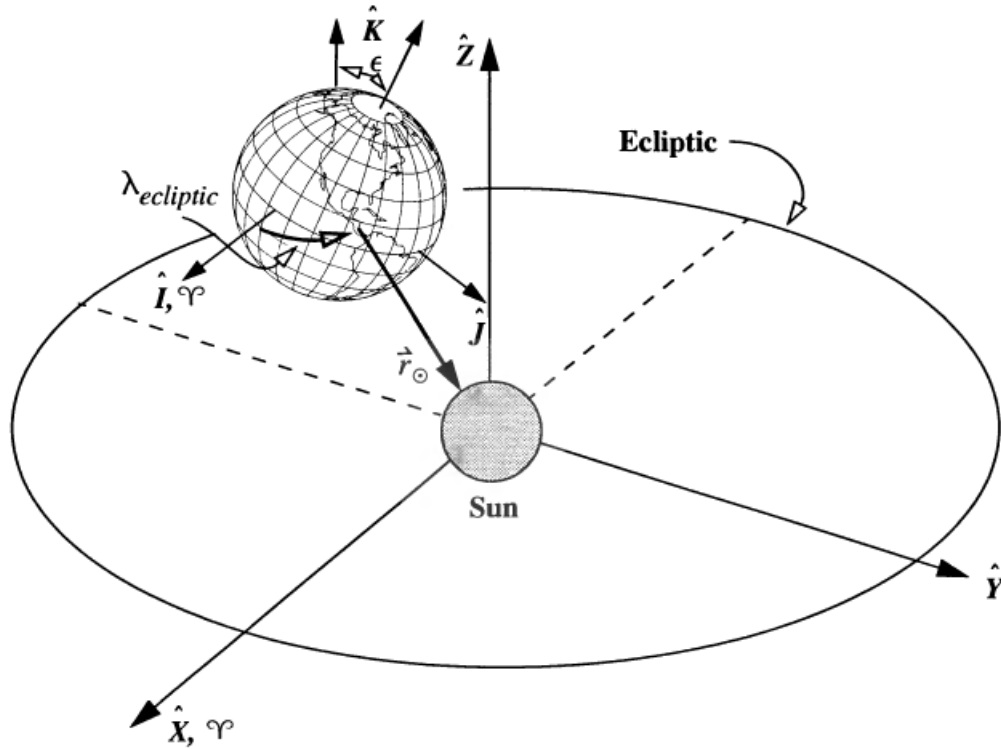


Figure 3.1 – Sun Position Vector. Source: Vallado (1997)

3.1.3 ASTRONOMICAL ALMANAC MODEL

This model, presented in the Astronomical Almanac 2015 provides the apparent position of the Sun with a precision of 1'. This model utilizes the Julian Date (JD) as well.

The time argument (n) is the number of days of TT (Terrestrial Time) from J2000.0. Universal Time (UT) can be used instead of TT neglecting the error:

$$n = JD - 2451545.0 \quad (3.30)$$

The mean longitude is given as

$$\lambda_M = 280.460^\circ + 0.9856474n \quad (3.31)$$

The mean anomaly is given as

$$M = 357.528^\circ + 0.9856003n \quad (3.32)$$

The ecliptic longitude and the ecliptic latitude are given as

$$\lambda_{ecliptic} = \lambda_M + 1.915^\circ \sin M + 0.020 \sin 2M \quad (3.33)$$

$$\beta_{ecliptic} = 0^\circ \quad (3.34)$$

The obliquity of ecliptic is given as

$$\epsilon = 23.439^\circ - 0.0000004n \quad (3.35)$$

The distance of the Sun from Earth, r , in Astronomical Units:

$$r = 1.0014 - 0.01671 \cos M - 0.00014 \cos 2M \quad (3.36)$$

Finally, the equatorial rectangular coordinates of the Sun, in AU, can be determined by the following equations:

$$x = r \cos \lambda_{ecliptic} \quad (3.37)$$

$$y = r \cos \epsilon \sin \lambda_{ecliptic} \quad (3.38)$$

$$z = r \sin \epsilon \sin \lambda_{ecliptic} \quad (3.39)$$

3.1.4 CONSIDERATIONS

The differences between the three models are listed below:

- The NanosatC-BR2 model considers that the distance from Earth to the Sun is 1 Astronomical Unit, but the other two models consider that this distance varies with the mean anomaly. Therefore, the NanosatC-BR2 model performs less calculations.

- In the NanosatC-BR2 model, the ecliptic longitude depends on the mean anomaly (M) and on the argument of perihelion (w). On the other hand, the ecliptic longitude of other two models depend on the mean anomaly (M) and on the mean longitude (λ_M). However, the mean longitude can be written in terms of mean anomaly (M) and argument of perihelion (w):

$$\lambda_M = M + \varphi \quad (3.40)$$

But,

$$\varphi = N + w \quad (3.41)$$

The longitude of the ascending node (N) is zero as explained in section 2.4. Therefore:

$$\lambda_M = M + w \quad (3.42)$$

3.2 MAGNETIC FIELD VECTOR

The International Geomagnetic Reference Field (IGRF) is a series of mathematical models that describe the Earth's Magnetic Field. The IGRF12 is the twelfth and latest generation of the IGRF, which was released by the International Association of Geomagnetism and Aeronomy (IAGA) in December 2014 (Thébault et al, 2014). Several institutes and scientists around the world provided magnetic field data for the conception of this model. In Brazil, for example, the National Observatory based in Rio de Janeiro, was one of the contributors.

3.2.1 MATHEMATICAL MODEL – IGRF12

The magnetic field (\vec{B}) on the Earth's surface and above it can be written in terms of magnetic scalar potential:

$$\vec{B} = -\nabla V \quad (3.43)$$

In spherical polar coordinates, V can be approximated by the following finite series:

$$V(r, \theta, \phi, t) = a \sum_{n=1}^N \left(\frac{a}{r}\right)^{n+1} \sum_{m=0}^n [g_n^m(t) \cos(m\phi) + h_n^m(t) \sin(m\phi)] P_n^m(\theta) \quad (3.44)$$

Where r is the radial distance from the center of the Earth, a is the Earth's mean reference radius (6,371.2 km), θ is the colatitude and ϕ is the east longitude from the Greenwich Meridian. The functions $P_n^m(\theta)$ are the Schmidt quasi-normalized associated Legendre function of degree n , and order m . Finally, g_n^m and h_n^m are the Gauss coefficients given in nanotesla (nT). According to Thébault et al (2015), these coefficients “are provided for the main field (MF) at epochs separated by 5 years between 1900.0 and 2015.0 A.D.”, and they are given as:

$$g_n^m(t) = g_n^m(T_0) + \dot{g}_n^m(T_0) \cdot (t - T_0) \quad (3.45)$$

$$h_n^m(t) = h_n^m(T_0) + \dot{h}_n^m(T_0) \cdot (t - T_0) \quad (3.46)$$

The model above is valid from 1900.0 to 2020.0.

The unit of the first derivatives above is nT/year. t is the time in units of year and T_0 is the epoch preceding t .

If the MF models exist for both T_0 and $T_0 + 5$, $\dot{g}_n^m(T_0)$ is written as

$$\dot{g}_n^m(T_0) = \frac{[g_n^m(T_0 + 5) - g_n^m(T_0)]}{5.0} \quad (3.47)$$

For the final 5 years of the IGRF12 validity, the coefficients \dot{g}_n^m and \dot{h}_n^m of the average secular variation are provided. In Thébault et al (2015), it is possible to verify the values for g and h for different values of n and m .

Finally, the components of the geomagnetic field in geocentric coordinates (terrestrial Cartesian) are given as follows:

$$X = \frac{1}{r} \frac{\partial V}{\partial \theta}, \quad Y = -\frac{1}{r \sin \theta} \frac{\partial V}{\partial \phi}, \quad Z = \frac{\partial V}{\partial r} \quad (3.48)$$

Where X is the north component, Y is the east component and Z is the vertical component (Figure 3.1).

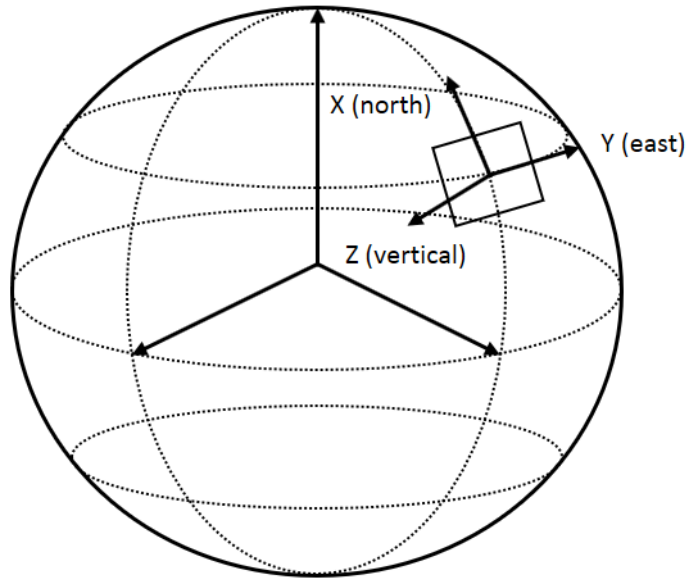


Figure 3.1 – North component (X), east component (Y) and vertical component (Z) of the magnetic field.

As is can be seen in the figure above, X points to north (positive northward), and Z points toward the interior of the Earth (positive downward) and Y points to east completing the right-handed coordinate system (positive eastward).

The model utilized by the NanosatC-BR2 is truncated for $n=m=5$. In the next chapter, this truncated model will be compared to the maximum truncation degree model ($n=m=13$), provided by the British Geological Survey in the United Kingdom (British Geological Survey, 2014).

3.3 ERROR ANALYSIS

This section will present the equations utilized to perform the comparison between the models throughout the error analysis.

Suppose that there are two sets of data known as Set 1 and Set 2, provided by the vectors $\mathbf{R}_1(x_1, y_1, z_1)$ and $\mathbf{R}_2(x_2, y_2, z_2)$. The magnitude of Set 1 is given as

$$\|\mathbf{R}_1\| = M_1 = \sqrt{(x_1^2) + (y_1^2) + (z_1^2)} \quad (3.49)$$

And the magnitude of Set 2 is given as

$$\|\mathbf{R}_2\| = M_2 = \sqrt{(x_2^2) + (y_2^2) + (z_2^2)} \quad (3.50)$$

The angle error between these two vectors are defined by

$$\theta = \cos^{-1} \frac{\mathbf{R}_1 \cdot \mathbf{R}_2}{\|\mathbf{R}_1\| \|\mathbf{R}_2\|} \quad (3.51)$$

The magnitude error (ME), in percentage, is given as

$$ME = 100 - \frac{M_1}{M_2} 100 \quad (3.52)$$

When you have a sample of n elements, the average of these elements can be calculated as follows:

$$\bar{x} = \frac{x_1 + x_2 + x_3 \dots + x_n}{n} \quad (3.53)$$

The standard deviation measures how precise this average is, and it is defined by (Weston, n. d.):

$$S = \frac{\sqrt{(x_1 - \bar{x})^2 + (x_2 - \bar{x})^2 + (x_3 - \bar{x})^2 + \dots + (x_n - \bar{x})^2}}{n - 1} \quad (3.54)$$

The average is more reliable when S is close to zero.

4 SOFTWARE ARCHITECTURE

The *Sistema de Determinação de Atitude Tolerante à Falhas* (SDTAF), the first attitude determination system developed in Brazil, is result of a cooperation between UFMG, INPE and UFABC. This system is based on a magnetometer and solar sensors which provide the attitude using the QUEST algorithm. The software to determine the attitude in terms of quaternions, developed by Dr. Helio Kuga (INPE) and Valdemir Carrara (INPE) using C programming language, is divided into several modules which are represented in Figure 4.1. Each module is listed as follows:

- i. **main.c**: this is the main code of the software. The inputs of this code are the MJD, the time of the day in seconds, the Two-Line Element (TLE), the magnetometer vector, in Tesla, and the sun sensor vector. This code calls functions of the other modules, and the outputs are the quaternions and the state vector. For more details about the TLE, refer to section 4.1.
- ii. **sdatf_igrf.c**: this module is the IGRF12 model truncated for $n=m=5$. For more details about the mathematical model, refer to section 3.2. The inputs are the year, distance from center of Earth (km), colatitude (degree) and east longitude (degree). The outputs are components of the magnetic vector in nano Tesla: north component, east component and vertical component.
- iii. **sdatf_eph_ref.c**: this module provides the magnetic vector in geocentric inertial coordinates.
- iv. **sdatf_matrices.c**: this module is a library of functions which execute computations related to matrices and vectors. For example, this library has functions

that get the dot product, the scalar product of two vectors, computes the result of the sum of two matrices, etc.

- v. `sdatf_attaux.c`:** this module is a library of functions which computes the rotation matrix about an axis, given the angle of rotation about this axis.
- vi. `sdatf_orbit.c`:** this code is a library of functions utilized by other modules. For example, this code provides a code utilized by `ita_eph_ref.c` that transforms geocentric terrestrial coordinates into geocentric inertial coordinates.
- vii. `sdatf_sun_dir.c`:** this module calculates the direction vector of the sun in the geocentric inertial system, according to Section 3.1.1.
- viii. `sdatf_det_est`:** this module contains the QUEST algorithm.
- ix. `spg4.c`:** this module provides the SPG4 model, which propagates analytically the satellite orbit. The input is the TLE and the time in minutes between the information provided by the onboard computer and the TLE. The output is the state vector in meters (position vector) and in meters per seconds (velocity vector). Although this code is part of the attitude determination software, and its outputs are used for the attitude determination, this work will not explain in details this model.

Software Architecture (Draft 1)

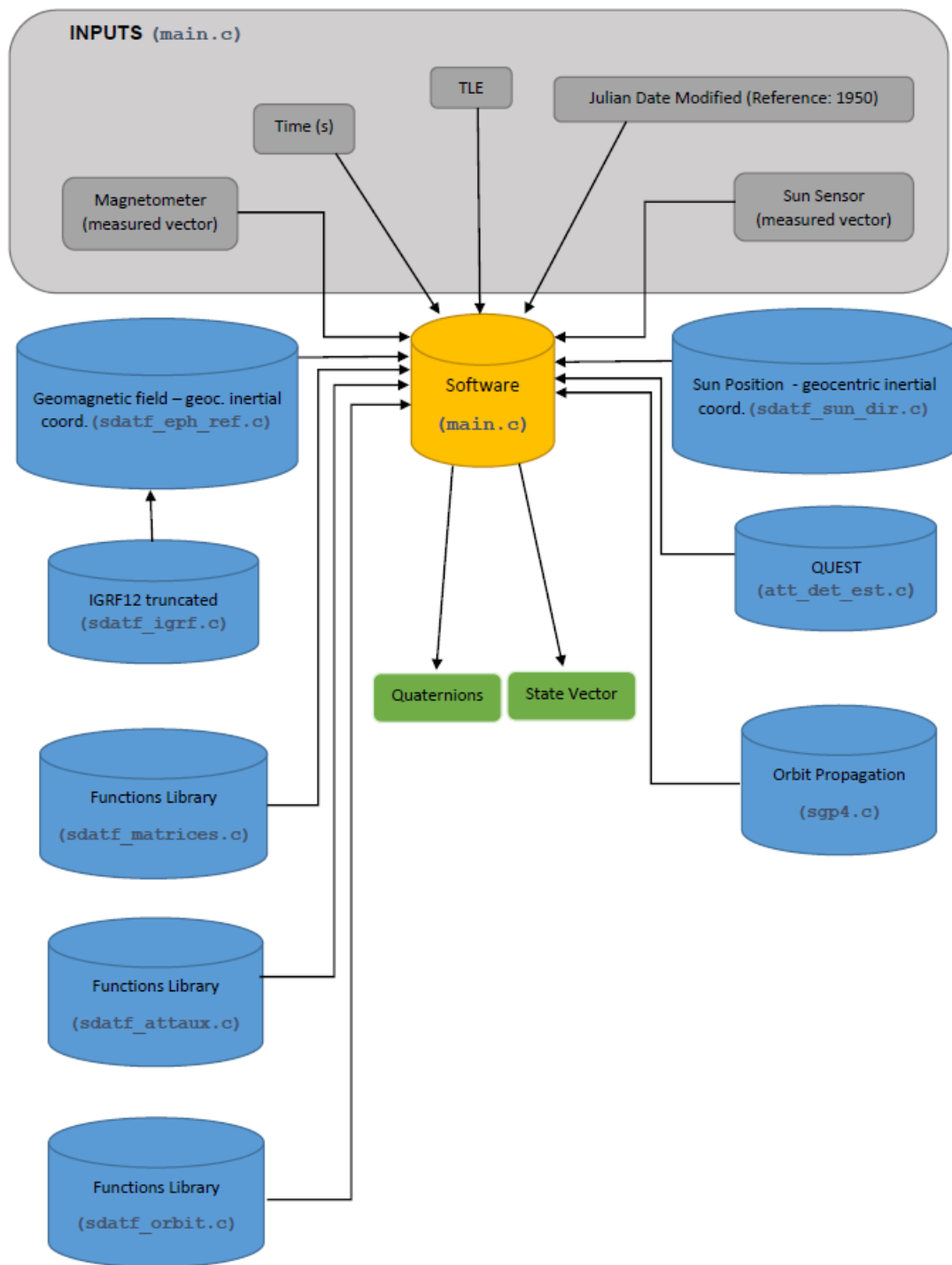


Figure 4.1 – Software Architecture

4.1 TWO-LINE ELEMENT (TLE)

TLE is a set of data which provides information about the orbit of a given satellite (Figure 4.2), and it is one of the main inputs of the attitude determination software.

1	NANOSATC-BR1		4	5	6	7	8	9	10
1	40024U	14033Q		15289.69306111	.00001566	00000-0	17660-3	0	9994
2	40024	97.9404		190.2884	0013434	139.9546	220.2663	14.87970572	71862
2	3	11		12	13	14	15	16	17

Figure 4.2 – TLE of the NANOSATC-BR1 as per 17 October 2015.

The figure above shows the TLE of the NanosatC-BR1, and as the name suggests, the information is provided through two lines. Each piece of information is enumerated as follows (NASA, 2011):

- (1) **Name of the Satellite:** name of the satellite (NANOSAC-BR1);
- (2) **Line number:** line number of the TLE (1 or 2);
- (3) **Satellite Number:** number assigned by the United States Space Command (USSPACECOM) for each artificial satellite orbiting earth. This number is also known as NORAD Catalog Number, NASA catalog number or USSPACECOM object number. In this example, the satellite number is 40024. The letter “U” stands for Unclassified, and it is related to the security information of the data, that is, the satellite is an unclassified object.
- (4) **International Designator:** The two first digits are the year of the launch, the next three digits are the launch number of the year, and the alphabetical characters provide the information about the piece of the given launch. For example, the first piece of a launch is denoted by “A”, the second piece is denoted by B, and so on. However, the letters “I” and “O” are not used. The 25th piece is denoted by “AA”, the 26th piece is denoted by “AB”, and so on. After “AZ” comes “BA”, “BB”, “BC”, etc. In the example below, the International Designator is “14033Q”, which means that the satellite was launched in 2014, and it was the 33th launch of that year. Moreover, the alphabetical letter “Q” means that this satellite was the 7th object resulting from this launch.
- (5) **Epoch (year and day of the year):** this number provides information about the year, day and time of the TLE set. The first two digits represent the last two digits of a given year called

epoch year. For example, in the example below, the epoch year is 2015. The remaining numbers represent the continuous amount of time measured in days from the epoch January 1, 2015 (0.0 UT – midnight between December 31, 2014 and January 1, 2015). For example, in the example below this number is 289.69306111, which means that 289 days has passed since January 1, 2015, therefore, the day that this TLE was collected is November 17, 2015. Finally, 0.69306111 can be transformed into hours, minutes and seconds to provide the time that this TLE was collected.

(6) First Derivative of the Mean Motion: this element represents the 1st derivative of the mean motion divided by 2, in units of revolutions per day².

(7) Second Derivative of the Mean Motion: this element represents the 2st derivative of the mean motion divided by 6, in units of revolutions per day³.

(8) BSTAR Drag Term (B^*): this term is given in units of inverse Earth Radii, and it is defined as

$$B^* = \frac{B\rho_0}{2} \quad (4.1)$$

Where ρ_0 is the atmospheric density (kg/m³) and B is the ballistic coefficient given in units of area per mass. B can be written as follows

$$B = \frac{C_D A}{M} \quad (4.2)$$

Where C_D is the coefficient drag, A is the cross-sectional area of the satellite and M is the satellite mass.

(9) Ephemeris Type: this element identifies the orbital model utilized to provide the data. All distributed TLEs have a value of zero, which means that the data was generated using the SGP4 for near-Earth satellites or SDP4 for deep-space satellites (Hoots and Roerich, 1980).

(10) Element Number & Check Sum: the first 3 digits of this number is the element number, which is a continuous count of all TLEs generated by USSPACECOM for this object. For example, in the example above, it is possible to verify that the element number is 999, which is the maximum number allowed, therefore this may be the 999th TLE generated by USSPACECOM. The next number after 999 is 1, and the count starts all over again.

The check sum is the sum of all numbers in the line, and assigning the value of 1 to every minus sign. In the example below, this sum of numbers and minus signs is 144, therefore the last digit of this sum is the checksum. For example, the checksum in the example below is 4.

(11) Inclination: this number is the inclination of the object's orbit, in degrees. In the example below, the inclination of the orbit is 97.9404° .

(12) Right Ascension of the Ascending Node: this number is the RAAN, in degrees. In the example below, the RAAN is 190.2884° .

(13) Eccentricity: this number is the eccentricity of the object's orbit, in degrees. In the example below, the eccentricity of the orbit is 0.013434, which means that the object has an elliptical orbit.

(14) Argument of Perigee: this number is the argument of perigee of the object's orbit, in degrees. In the example below, the argument of perigee of the orbit is 139.9546° .

(15) Mean Anomaly: this number is the mean anomaly of the object's orbit, in degrees. In the example below, the mean anomaly of the orbit is 220.2663° .

(16) Mean Motion: this is the mean number of orbits that the object completes per day.

(17) Revolution Number at Epoch & Checksum: the first four digits of this element the orbit number at the epoch time. According to Sumus Technology (2016), "the period from launch to the first ascending node is considered to be revolution 0 and revolution 1 begins when the first ascending node is reached". In the example below the revolution number is 7168. The last digit of this number is the checksum of the second line, for example, the sum of all values of this line is 122, therefore the checksum is 2.

4.2 ATTITUDE DETERMINATION

In this section, the steps to determine the quaternions will be explained in details. As described before, the inputs of the software are the Two Line Elements, the time of the day in seconds (fd), the Modified Julian Date, the measured vector of the magnetometer in nanoTesla (\widehat{W}_m), and the measured vector of the sun sensor (\widehat{W}_s). The attitude is determined using the QUEST algorithm, so four vectors are needed: two measured vectors in the body frame (\widehat{W}_m and \widehat{W}_s), and two vectors in the inertial frame (\widehat{V}_m and \widehat{V}_s).

The sun position vector in the inertial frame \widehat{V}_s is determined directly from the NanoSatC-BR2 model explained in Section 3.1.1. On the other hand, the magnetic field vector

in the inertial frame ($\hat{\mathbf{V}}_m$) is determined after some transformations, that is, the vector determined by the IGRF12 model is in terrestrial cartesian coordinates.

The steps to determine the quaternions are listed below:

STEP 1: Calculate the Greenwich Mean Sideral Time (Module: sdatf_orbit.c)

First, it is necessary to determine the Greenwich Mean Sideral Time (GMST) in radians referred to J2000 using the following software inputs: Modified Julian Date and fraction of the day in seconds (fd). The equations for these calculations are presented in Section 2.5.2.

STEP 2: Calculate the position vector in meters (Module: sgp4.c)

This step utilizes the SPG4 to determine the position vector ($\mathbf{P}_{inertial}$) in meters (Geocentric Inertial Position Coordinates). Herein, this module will not be explained in details.

STEP 3: Transformation into Geocentric Terrestrial Coordinates (Module: sdatf_orbit.c)

Now, it is necessary to transform the position vector from geocentric inertial coordinates ($\mathbf{P}_{inertial}$) to geocentric terrestrial coordinates ($\mathbf{P}_{terrestrial}$). For this, a rotation about the z axis is necessary:

$$\mathbf{P}_{terrestrial} = \begin{bmatrix} \cos(GMST) & \sin(GMST) & 0 \\ -\sin(GMST) & \cos(GMST) & 0 \\ 0 & 0 & 1 \end{bmatrix} \begin{bmatrix} m \\ n \\ s \end{bmatrix} = \begin{bmatrix} M \\ N \\ S \end{bmatrix} \quad (4.3)$$

$$\text{Where } \mathbf{P}_{inertial} = \begin{bmatrix} m \\ n \\ s \end{bmatrix}.$$

STEP 4: Transformation into Geocentric Spherical Coordinates (Module: sdatf_orbit.c)

It is necessary to get the position vector in geocentric spherical coordinates in terms of terrestrial longitude (ϕ_{long}) in radian, geocentric latitude (λ_{lat}) in radians and geocentric distance d in meters:

$$\phi_{long} = \tan^{-1} \left(\frac{N}{M} \right) \quad (4.4)$$

$$d = \|\mathbf{P}_{terrestrial}\| \quad (4.5)$$

$$\lambda_{lat} = \sin^{-1} \left(\frac{S}{d} \right) \quad (4.6)$$

STEP 5: Calculate the inputs of the IGRF12 model (Module: sdatf_iph_ref.c)

The inputs of the IGRF12 is the distance from the center of the Earth (d), the east longitude (ϕ), which ranges from 0° to 360° , the colatitude (θ), which ranges from 0° to 180° , and the fraction of the year (t).

Note that d , given in meters, can be considered the radial distance from the center of the Earth. It is necessary to divide this value per 1000 to get it in km:

$$r = \frac{d}{1000} \quad (4.7)$$

It is possible to write that the east longitude (ϕ) is equal the east longitude (ϕ) plus 360° :

$$\phi = \phi_{long} + 360^\circ \quad (4.8)$$

Moreover, the colatitude (θ) can be written in terms of geocentric latitude:

$$\theta = \frac{\pi}{2} - \lambda_{lat} \quad (4.9)$$

Finally, the time (fraction of the year) is given as:

$$t = 2015 + \frac{MJD - 23741}{TropYear} \quad (4.10)$$

Where $TropYear$ is the Tropical Year that equals 365.24210979 days.

Note that 23741 is the MJD for 1st January, 2015.

STEP 6: Calculate the magnetic field vector (Module: `sdatf_igrf.c`)

Now that all inputs of the IGFR12 model was obtained, magnetic field vector shall be calculated using the model presented in section 3.2. Therefore, the following components of the magnetic field vector can be determined in Tesla: north component (X), east component (Y) and vertical component (Z). These three components form the vector \mathbf{B} .

STEP 7: Rotation matrix (Module: `sdatf_eph_ref.c`)

Now it is necessary to perform two rotations: one rotation about the y axis and another rotation about the z axis.

First rotation about the y axis by the angle $\frac{\pi}{2} + \theta$:

$$\mathbf{B}_y = \begin{bmatrix} \cos\left(\frac{\pi}{2} + \theta\right) & 0 & -\sin\left(\frac{\pi}{2} + \theta\right) \\ 0 & 1 & 0 \\ \sin\left(\frac{\pi}{2} + \theta\right) & 0 & \cos\left(\frac{\pi}{2} + \theta\right) \end{bmatrix} \begin{bmatrix} X \\ Y \\ Z \end{bmatrix} \quad (4.11)$$

Where $\mathbf{B} = \begin{bmatrix} X \\ Y \\ Z \end{bmatrix}$.

Second rotation about the y axis by the angle $-\phi_{long}$:

$$\mathbf{B}_{y,z} = \begin{bmatrix} \cos(-\phi_{long}) & \sin(-\phi_{long}) & 0 \\ -\sin(-\phi_{long}) & \cos(-\phi_{long}) & 0 \\ 0 & 0 & 1 \end{bmatrix} \mathbf{B}_y \quad (4.12)$$

STEP 8: Transformation into Geocentric Inertial Coordinates (Module: `sdatf_eph_ref.c`)

Finally, the magnetic field vector shall be transformed from terrestrial cartesian coordinates to geocentric inertial coordinates:

$$\mathbf{B}_m = \begin{bmatrix} \cos(-GMST) & \sin(-GMST) & 0 \\ -\sin(-GMST) & \cos(-GMST) & 0 \\ 0 & 0 & 1 \end{bmatrix} \mathbf{B}_z \quad (4.13)$$

STEP 9: Calculate the unit vector of \mathbf{B}_m (Module: sdatf_matrices.c)

The unit vector is calculated as follows:

$$\hat{\mathbf{V}}_m = \frac{\mathbf{B}_m}{\|\mathbf{B}_m\|} \quad (4.14)$$

$$\hat{\mathbf{W}}_m = \frac{\mathbf{W}_m}{\|\mathbf{W}_m\|} \quad (4.15)$$

STEP 10: Calculate the sun position vector (Module: sdatf_sun_dir.c)

The sun position vector $\hat{\mathbf{V}}_s$, which is a unit vector, is obtained directly from the sun position model presented in section 3.1.1.

STEP 11: Determine the quaternions (Module: att_det_est.c)

Finally, after obtaining the desired vectors ($\hat{\mathbf{W}}_m, \hat{\mathbf{W}}_s, \hat{\mathbf{V}}_m, \hat{\mathbf{V}}_s$), the attitude is determined in the form of quaternions using the QUEST algorithm presented in section 2.3.4.

5 SIMULATION & ERROR ANALYSIS

This chapter presents the simulation results of the attitude determination software, and also presents the results of the error analysis of the sun position vector and the magnetic field vector in the inertial frame.

5.1 SIMULATION RESULTS: ATTITUDE DETERMINATION

5.1.2 SIMULATION 1

This simulation considers a 3-1-3 sequence of Euler rotation, and the Euler Angles are given as follows:

$$\theta_p = 10^\circ$$

$$\theta_y = 20^\circ$$

$$\theta_r = 30^\circ$$

Where θ_y is the yaw angle, θ_r is the roll angle and θ_p is the pitch angle.

It is possible to write the rotation matrix in terms of Euler Angles. For example, for a 3-1-3 sequence, we have:

$$A_{313}(\theta_y, \theta_r, \theta_p) = A_3(\theta_p) \cdot A_1(\theta_r) \cdot A_3(\theta_y) \quad (5.1)$$

We define a rotation of θ_p about the z-axis, a rotation of θ_r about the x-axis and a rotation of θ_y about the z-axis as follows:

$$A_3(\theta_p) = \begin{bmatrix} \cos(\theta_p) & \sin(\theta_p) & 0 \\ -\sin(\theta_p) & \cos(\theta_p) & 0 \\ 0 & 0 & 1 \end{bmatrix}$$

$$A_1(\theta_r) = \begin{bmatrix} 1 & 0 & 0 \\ 0 & \cos(\theta_r) & -\sin(\theta_r) \\ 0 & \sin(\theta_r) & \cos(\theta_r) \end{bmatrix} \quad (5.2)$$

$$A_3(\theta_y) = \begin{bmatrix} \cos(\theta_y) & \sin(\theta_y) & 0 \\ -\sin(\theta_y) & \cos(\theta_y) & 0 \\ 0 & 0 & 1 \end{bmatrix}$$

Therefore, substituting Equations 5.2 into Equation 5.1:

$$A = \begin{bmatrix} \cos(\theta_p)\cos(\theta_y) - \sin(\theta_p)\cos(\theta_r)\sin(\theta_y) & \cos(\theta_p)\sin(\theta_y) + \sin(\theta_p)\cos(\theta_r)\cos(\theta_y) & \sin(\theta_p)\sin(\theta_r) \\ -\sin(\theta_p)\cos(\theta_y) - \cos(\theta_p)\cos(\theta_r)\sin(\theta_y) & -\sin(\theta_p)\sin(\theta_y) + \cos(\theta_p)\cos(\theta_r)\cos(\theta_y) & \cos(\theta_p)\sin(\theta_r) \\ \sin(\theta_r)\sin(\theta_y) & -\sin(\theta_r)\cos(\theta_y) & \cos(\theta_r) \end{bmatrix} \quad (5.3)$$

Hence, substituting the angles into the equation above, we get the following rotation matrix:

$$A = \begin{bmatrix} 0.8740 & 0.4781 & 0.0868 \\ -0.4549 & 0.7420 & 0.4924 \\ 0.1710 & -0.4698 & 0.8660 \end{bmatrix} \quad (5.4)$$

Using Equation (2.1) to calculate the sun position vector and the magnetometer in the satellite frame:

$$\widehat{W}_s = A \widehat{V}_s = \begin{bmatrix} -0.4430 \\ 0.8762 \\ -0.1897 \end{bmatrix} \quad (5.5)$$

$$\widehat{W}_m = A \widehat{V}_m = \begin{bmatrix} 0.0364 \\ 0.9229 \\ 0.3832 \end{bmatrix} \quad (5.6)$$

Where \widehat{V}_s and \widehat{V}_m is the unit vector of the sun position and the unit vector of the magnetic field, in the inertial frame for the time and date of this simulation (Table 5.1). These vectors were calculated using the mathematical models described in Chapter 3.

Table 5.1 – Simulation 1 Inputes

INPUT	VALUE
fd (seconds)	12345.6
MJD (days)	23970
\widehat{W}_m	$0.0364 \mathbf{i} + 0.9229 \mathbf{j} + 0.3832 \mathbf{k}$
\widehat{W}_s	$-0.4430 \mathbf{i} + 0.8762 \mathbf{j} - 0.1897 \mathbf{k}$

Additionally to the inputs in Table 5.1, the following TLE was also used as input in the simulation:

NANOSATC-BR1

1 40024U 14033Q 15227.21713877 .00001026 00000-0 11838-3 0 9997
2 40024 97.9460 127.7226 0012743 357.5960 2.5192 14.87803168 62571

Using the \widehat{W}_s and \widehat{W}_m as input of the software, we get the quaternions in Table 5.2.

Table 5.2 – Simulation 2 Outputs

OUTPUT	VALUE
$GMST$ (degree)	17.623417
$P_{inertial}$ (m)	$2291774 \mathbf{i} - 3928348.75 \mathbf{j} - 5313940.5 \mathbf{k}$
$P_{terrestrial}$ (m)	$994869.5 \mathbf{i} - 4437836 \mathbf{j} - 5313940.5 \mathbf{k}$
r (km)	6994.435059
ϕ (degree)	282.635605
θ (degree)	139.441132
B (nTesla)	$2079.958008 \mathbf{i} - 679.360229 \mathbf{j} + 44009.472656 \mathbf{k}$
$B_{y,z}$ (Tesla)	$-0.000007 \mathbf{i} - 0.000026 \mathbf{j} + 0.000035 \mathbf{k}$
B_m (Tesla)	$0.000014 \mathbf{i} - 0.000023 \mathbf{j} + 0.000035 \mathbf{k}$
\widehat{V}_m	$-0.322498 \mathbf{i} + 0.522201 \mathbf{j} + 0.789494 \mathbf{k}$
\widehat{V}_s	$-0.818190 \mathbf{i} + 0.527512 \mathbf{j} + 0.228682 \mathbf{k}$
q	$0.257835 \mathbf{i} + 0.022534 \mathbf{j} + 0.249993 \mathbf{k}$
q_4	0.933015

The main output of the software are the quaternions, which will be compared to the quaternions of the attitude determination system of the NanosatC-Br2, in order to validate the SDATF in space. The quaternions found can be used to write the rotation matrix (Equation 2.4), and the result is given as follows:

$$\mathbf{A} = \begin{bmatrix} 0.8757 & 0.4786 & 0.0868 \\ -0.4553 & 0.7437 & 0.4929 \\ 0.1710 & -0.4703 & 0.8677 \end{bmatrix} \quad (5.7)$$

The result above is approximate to the result of Equation 5.4.

5.1.2 SIMULATION 2

This simulation considers a 3-1-2 sequence of Euler rotation, and the Euler Angles are the following:

$$\theta_p = 10^\circ$$

$$\theta_y = 20^\circ$$

$$\theta_r = 30^\circ$$

Where θ_y is the yaw angle, θ_r is the roll angle and θ_p is the pitch angle.

It is possible to write the rotation matrix in terms of Euler Angles. For example, for a 3-1-2 sequence, we have:

$$A_{312}(\theta_y, \theta_r, \theta_p) = A_2(\theta_p) \cdot A_1(\theta_r) \cdot A_3(\theta_y) \quad (5.8)$$

We define a rotation of θ_p about the x-axis, a rotation of θ_r about the x-axis and a rotation of θ_y about the z-axis as follows:

$$A_2(\theta_p) = \begin{bmatrix} \cos(\theta_p) & 0 & -\sin(\theta_p) \\ 0 & 1 & 0 \\ \sin(\theta_p) & 0 & \cos(\theta_p) \end{bmatrix}$$

$$A_1(\theta_r) = \begin{bmatrix} 1 & 0 & 0 \\ 0 & \cos(\theta_r) & -\sin(\theta_r) \\ 0 & \sin(\theta_r) & \cos(\theta_r) \end{bmatrix} \quad (5.9)$$

$$A_3(\theta_y) = \begin{bmatrix} \cos(\theta_y) & \sin(\theta_y) & 0 \\ -\sin(\theta_y) & \cos(\theta_y) & 0 \\ 0 & 0 & 1 \end{bmatrix}$$

Therefore, substituting Equations 5.9 into Equation 5.8:

$$A = \begin{bmatrix} \cos(\theta_p)\cos(\theta_y) - \cos(\theta_p)\cos(\theta_r)\cos(\theta_y) & \cos(\theta_p)\sin(\theta_y) + \sin(\theta_p)\cos(\theta_r)\cos(\theta_y) & -\sin(\theta_p)\cos(\theta_r) \\ -\cos(\theta_r)\sin(\theta_y) & \cos(\theta_r)\cos(\theta_y) & \sin(\theta_r) \\ \sin(\theta_p)\cos(\theta_y) + \cos(\theta_p)\sin(\theta_r)\sin(\theta_y) & \sin(\theta_p)\sin(\theta_y) - \cos(\theta_p)\sin(\theta_r)\cos(\theta_y) & \cos(\theta_p)\cos(\theta_r) \end{bmatrix} \quad (5.10)$$

Hence, substituting the angles into the equation above, we get the following rotation matrix:

$$A = \begin{bmatrix} 0.8957 & 0.4184 & -0.1504 \\ -0.2962 & 0.8138 & -0.5000 \\ 0.3316 & -0.4033 & 0.8529 \end{bmatrix} \quad (5.11)$$

Using Equation (2.1) to calculate the sun position vector and the magnetometer in the satellite frame:

$$\widehat{W}_s = A \widehat{V}_s = \begin{bmatrix} -0.5465 \\ 0.7860 \\ -0.2890 \end{bmatrix} \quad (5.12)$$

$$\widehat{W}_m = A \widehat{V}_m = \begin{bmatrix} -0.1891 \\ 0.9152 \\ 0.3558 \end{bmatrix} \quad (5.13)$$

Where \widehat{V}_s and \widehat{V}_m are the unit vector of the sun position and the unit vector of the magnetic field, in the inertial frame for the time and date of this simulation (Table 5.3). These vectors were calculated using the mathematical models described in Chapter 3.

Table 5.3 – Simulation 2 Inputs

INPUT	VALUE
fd (seconds)	12345.6
MJD (days)	23970
$\widehat{\mathbf{W}}_m$	$-0.1891 \mathbf{i} + 0.9152 \mathbf{j} + 0.3558 \mathbf{k}$
$\widehat{\mathbf{W}}_s$	$-0.5465 \mathbf{i} + 0.7860 \mathbf{j} - 0.2890 \mathbf{k}$

Using the $\widehat{\mathbf{W}}_s$ and $\widehat{\mathbf{W}}_m$ as input of the software, we get the quaternions in Table 5.4.

Table 5.4 – Simulation 2 Outputs

OUTPUT	VALUE
$GMST$ (degree)	17.623417
$\mathbf{P}_{inertial}$ (m)	$2291774 \mathbf{i} - 3928348.75 \mathbf{j} - 5313940.5 \mathbf{k}$
$\mathbf{P}_{terrestrial}$ (m)	$994869.5 \mathbf{i} - 4437836 \mathbf{j} - 5313940.5 \mathbf{k}$
r (km)	6994.435059
ϕ (degree)	282.635605
θ (degree)	139.441132
\mathbf{B} (nTesla)	$2079.958008 \mathbf{i} - 679.360229 \mathbf{j} + 44009.472656 \mathbf{k}$
$\mathbf{B}_{y,z}$ (Tesla)	$-0.000007 \mathbf{i} - 0.000026 \mathbf{j} + 0.000035 \mathbf{k}$
\mathbf{B}_m (Tesla)	$0.000014 \mathbf{i} - 0.000023 \mathbf{j} + 0.000035 \mathbf{k}$
$\widehat{\mathbf{V}}_m$	$-0.322498 \mathbf{i} + 0.522201 \mathbf{j} + 0.789494 \mathbf{k}$
$\widehat{\mathbf{V}}_s$	$-0.818190 \mathbf{i} + 0.527512 \mathbf{j} + 0.228682 \mathbf{k}$
\mathbf{q}	$0.239270 \mathbf{i} + 0.127695 \mathbf{j} + 0.189326 \mathbf{k}$
q_4	0.943716

The quaternions found can be used to write the rotation matrix (Equation 2.4), and the result is given as follows:

$$\mathbf{A} = \begin{bmatrix} 0.8584 & 0.4109 & -0.1453 \\ -0.2887 & 0.7765 & 0.4904 \\ 0.3265 & -0.3937 & 0.8155 \end{bmatrix} \quad (5.14)$$

The result above is approximate to the result of Equation 5.11.

5.1.3 SIMULATION 3

This simulation considers a 3-1-3 sequence of Euler rotation, and the Euler Angles are the following:

$$\theta_p = 0^\circ$$

$$\theta_y = 0^\circ$$

$$\theta_r = 0^\circ$$

Substituting these angles above into Equation 5.13, we get the following rotation matrix:

$$\mathbf{A} = \begin{bmatrix} 1 & 0 & 0 \\ 0 & 1 & 0 \\ 0 & 0 & 1 \end{bmatrix} \quad (5.15)$$

Using Equation (2.1) to calculate the sun position vector and the magnetometer in the satellite frame:

$$\widehat{\mathbf{W}}_s = \mathbf{A} \widehat{\mathbf{V}}_s = \begin{bmatrix} -0.818190 \\ 0.527512 \\ 0.228682 \end{bmatrix} \quad (5.16)$$

$$\widehat{\mathbf{W}}_m = \mathbf{A} \widehat{\mathbf{V}}_m = \begin{bmatrix} -0.322498 \\ 0.522201 \\ 0.789494 \end{bmatrix} \quad (5.17)$$

Where $\widehat{\mathbf{V}}_s$ and $\widehat{\mathbf{V}}_m$ are the unit vector of the sun position and the unit vector of the magnetic field, in the inertial frame for the time and date of this simulation (Table 5.5). These vectors were calculated using the mathematical models described in Chapter 3.

Table 5.5 – Simulation 3 Inputs

INPUT	VALUE
fd (seconds)	12345.6
MJD (days)	23970
\widehat{W}_m	$-0.322498 \mathbf{i} + 0.522201 \mathbf{j} + 0.789494 \mathbf{k}$
\widehat{W}_s	$-0.818190 \mathbf{i} + 0.527512 \mathbf{j} + 0.228682 \mathbf{k}$

Using the \widehat{W}_s and \widehat{W}_m as input of the software, we get the quaternions in Table 5.6. Note that the inputs and the outputs are the same because there is no rotation.

Table 5.6 – Simulation 3 Outputs

OUTPUT	VALUE
$GMST$ (degree)	17.623417
$P_{inertial}$ (m)	$2291774 \mathbf{i} - 3928348.75 \mathbf{j} - 5313940.5 \mathbf{k}$
$P_{terrestrial}$ (m)	$994869.5 \mathbf{i} - 4437836 \mathbf{j} - 5313940.5 \mathbf{k}$
r (km)	6994.435059
ϕ (degree)	282.635605
θ (degree)	139.441132
B (nTesla)	$2079.958008 \mathbf{i} - 679.360229 \mathbf{j} + 44009.472656 \mathbf{k}$
$B_{y,z}$ (Tesla)	$-0.000007 \mathbf{i} - 0.000026 \mathbf{j} + 0.000035 \mathbf{k}$
B_m (Tesla)	$0.000014 \mathbf{i} - 0.000023 \mathbf{j} + 0.000035 \mathbf{k}$
\widehat{V}_m	$-0.322498 \mathbf{i} + 0.522201 \mathbf{j} + 0.789494 \mathbf{k}$
\widehat{V}_s	$-0.818190 \mathbf{i} + 0.527512 \mathbf{j} + 0.228682 \mathbf{k}$
q	$0 \mathbf{i} + 0 \mathbf{j} + 0 \mathbf{k}$
q_4	0

The quaternions found can be used to write the rotation matrix (Equation 2.4), and the result is given as follows:

$$\mathbf{A} = \begin{bmatrix} 1 & 0 & 0 \\ 0 & 1 & 0 \\ 0 & 0 & 1 \end{bmatrix} \quad (5.18)$$

The result above is approximate to the result of Equation 5.15.

5.2 ERROR ANALYSIS: SUN POSITION VECTOR

The NanoSatC-BR2 model was compared to low precision models such as the Vallado's model (1997) and the Astronomical Almanac model (Defense Dept. Naval Observatory, 2014). These two last models were implemented using C language as well. Moreover, the NanoSatC-BR2 was compared to results given by the Systems Tool Kit (STK) software. This software was developed by the Analytical Graphics Inc (AGI), a company based in the US, and it provides modeling and simulation of aircraft, missiles and satellites missions (AGI, 2015). The software version utilized for the analysis is the tenth.

In Table 5.7, it is possible to verify the results of the error analysis. In order to perform this analysis, data was collected from every day of the 2015 year, and at the beginning of each day (0.0 hours). That is, sun position vectors were determined for each day of that year.

As it can be seen in Table 5.7, the vector magnitude of the Vallado's Model and Astronomical Almanac model is almost the same than the magnitude provided by the STK model because the Minimum Absolute Magnitude Error, Maximum Absolute Magnitude Error and Average Absolute Magnitude Error are approximate zero per cent in comparison with the STK model. On the other hand, the Average Absolute Magnitude Error of the NanosatC-BR2 model differs approximated 1 per cent from the other three models. Although the magnitude of the Vallado's and Astronomical Almanac vectors are almost the same than the magnitude of the STK model, the two previously models provide same results than the NanoSatC-BR2 model in terms of the angle error. For example, the Average Angle Error, in degrees, of the NanosatC-BR2, Vallado's and Astronomical Almanac Model, in comparison with STK results are respectively, 0.22° , 0.22° and 0.22° . The Maximum Error Angle are respectively 0.23° , 0.22° and 0.23° , whereas the Minimum Error Angle are respectively 0.22° , 0.21° and 0.21° . The Average Angle Error and the Maximum Angle error of the model of the Nanosatc-Br2 in comparison with the Vallado's and Astronomical Almanac Model is 0.01° , which is an expected result because these models are low precision models that determine the sun position vector in a similar way, as presented in section 3.1 Moreover, as all results of the standard deviation is close to zero, it means that the set of data is not so dispersed from its mean.

Table 5.7 – Error Analysis Results: Comparison between models

Type of Errors	NanosatC-Br2 vs STK 10	NanosatC-Br2 vs (Vallado, 1997) Model	NanosatC-Br2 vs Astronomical Almanac 2015	(Vallado, 1997) Model vs STK 10	Astronomical Almanac 2015 vs STK 10
Min. Absolute Magnitude Error (%)	0.0	0.00	0.00	0.00	0.10
Max. Absolute Magnitude Error (%)	1.70	1.70	1.80	0.00	0.10
Average Absolute Magnitude Error (%)	1.06	1.06	1.07	0.00	0.10
Min. Angle Error (Deg)	0.22	0.01	0.00	0.21	0.21
Maximum Angle Error (Deg)	0.23	0.01	0.01	0.22	0.23
Average Angle Error (Deg)	0.22	0.01	0.01	0.22	0.22
Standard Deviation of Angle Error	3.02E-03	5.02E-04	7.35E-04	2.68E-03	2.54E-03

The observations made before can be clarified through Figures 5.1, 5.2 and 5.3. In these figures, the angle error is plotted versus the day of the year, and the behavior of all models are similar to each other.

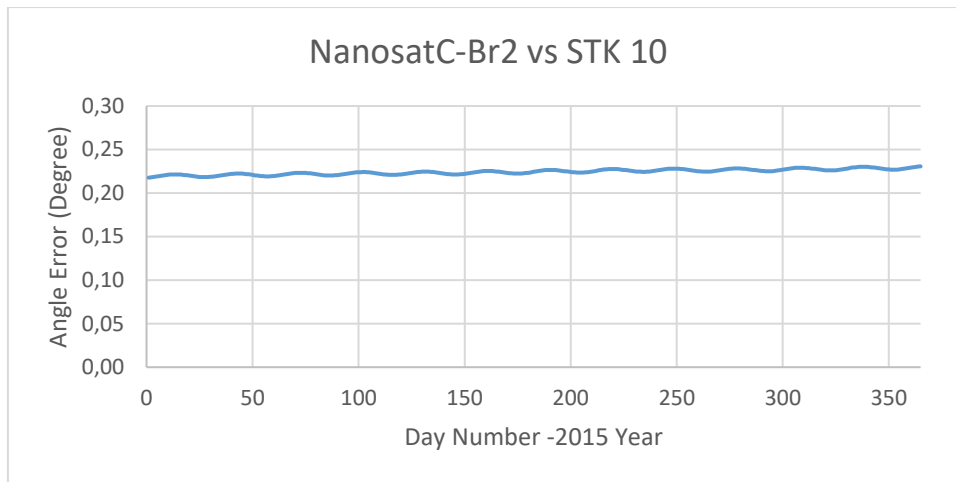


Figure 5.1 – Behavior of NanoSatC-Br2 in comparison with STK 10

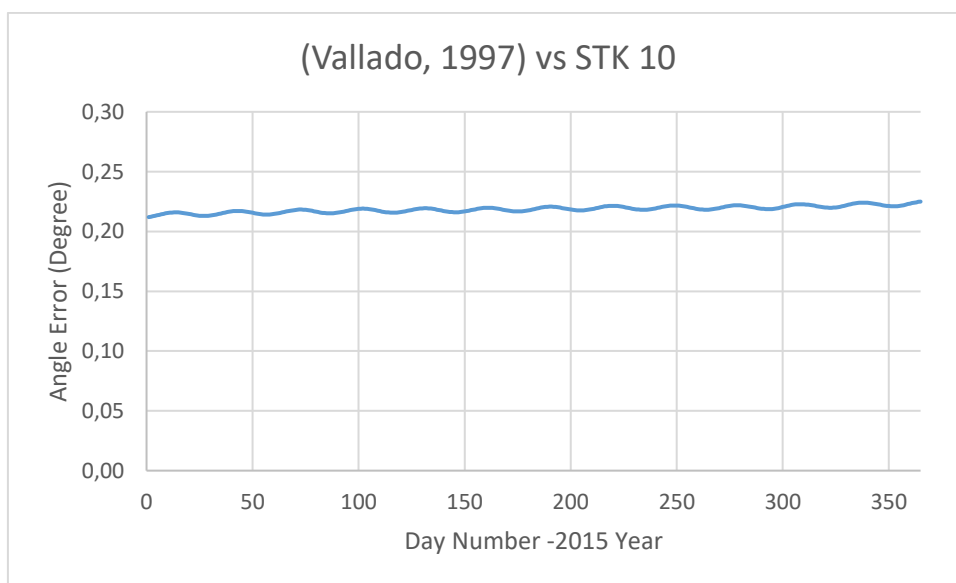


Figure 5.2 – Behavior of Vallado's model in comparison with STK 10

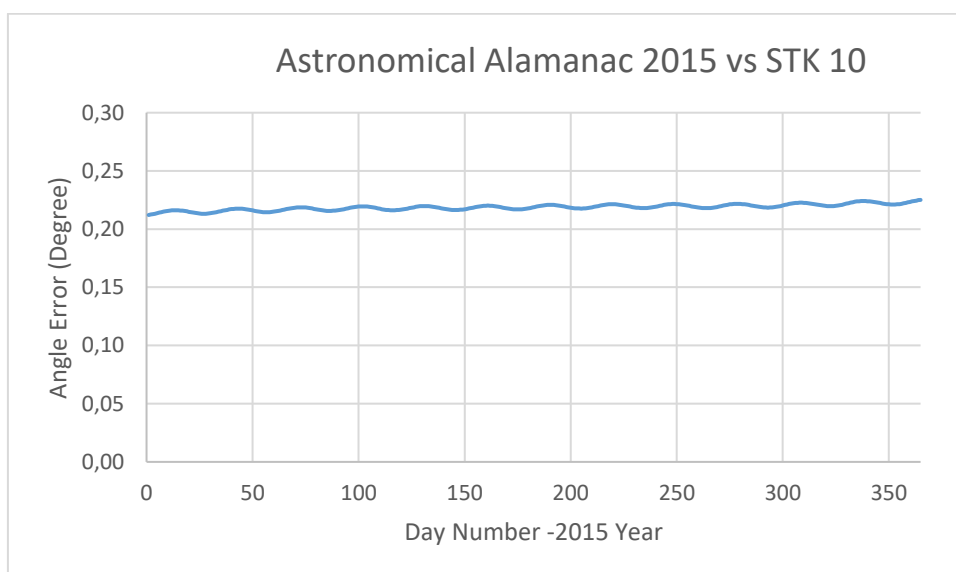


Figure 5.3 – Behavior of Astronomical Almanac model in comparison with STK 10

Moreover, the behavior of the NanosatC-BR2 in comparison to the Vallado's and Astronomical Almanac model is depicted in Figure 3.4 and 3.5.

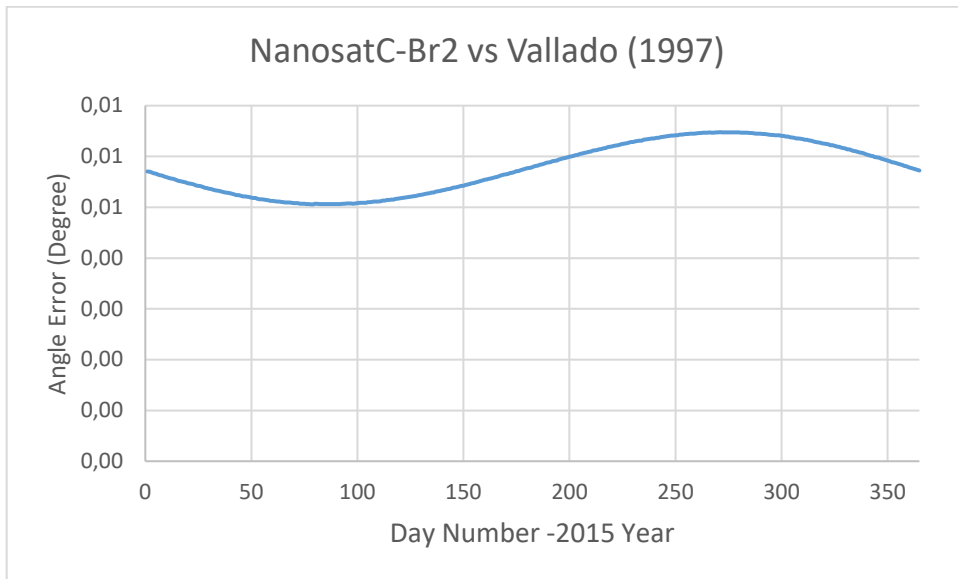


Figure 5.4 – Behavior of NanoSatC-Br2 in comparison with Vallado's Model

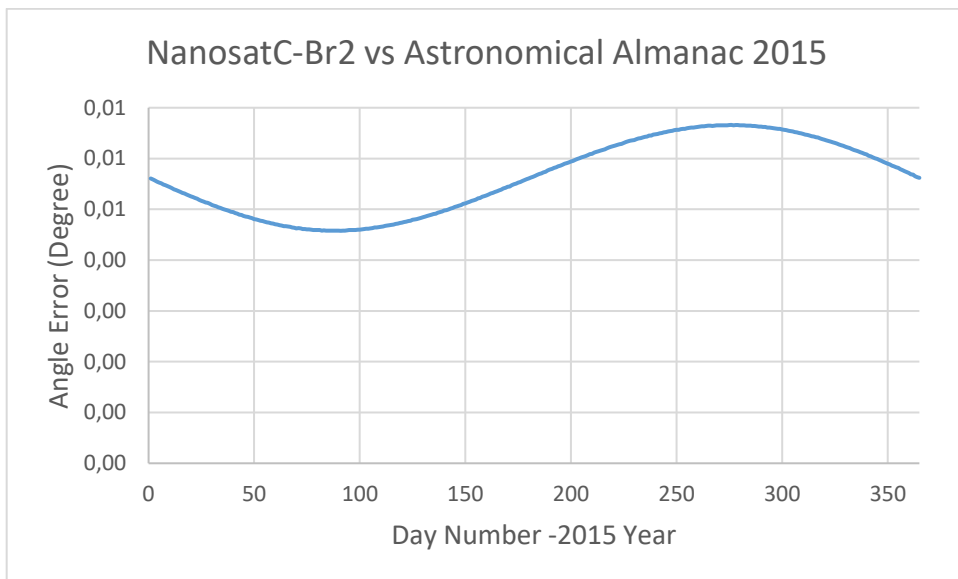


Figure 5.5 – Behavior of NanoSatC-Br2 in comparison with Astronomical Almanac 2015 model

It is important to observe that the models utilize different time standards, for example:

- a. NanosatC-BR2 model utilizes UT1 (Universal Time)
- b. STK model utilizes UTC (Coordinated Universal Time)

- c. Astronomical Almanac model is based on TT (Terrestrial Times), but considers that $TT \approx UT1$.
- d. David Vallado's model is based on TDB, but considers that $TDB \approx UT1$.

Therefore, it is possible to conclude that there is an error related to the time standards, even if the difference between them are a few seconds. For example, the difference between UT1 and UTC varies from -0.9 second to +0.9 seconds (Fisher, 1996). The difference between TT and UTC, as per 1st January 2016, is +67.64 seconds (Schlyter, 2010). According to Fisher (1996), the TDB is the same as TT, “except for relativistic corrections to move the origin to the solar system barycenter”, and these corrections are about 1.6 milliseconds. It is also important to note that the model of NanosatC-Br2, the Vallado's model and the Astronomical Almanac model are models of low precision once they make many considerations in order to facilitate the determination of the sun position vector. On the other hand, it is not possible to determine which model the STK utilized to determine the sun position vector, and as the three latest models obtained approximated the same results when compared to the STK'S results, it is possible to conclude that the software may utilize a model of higher or even lower precision.

In brief, the simulation of the sun position vector of NanoSatC-Br2 provided results approximated to other models, and therefore the model provides results according the expected. However, before analyzing the final model presented in section 3.1.1, a mistake was found in one of the equations of the original model, and this mistake will be explained in the next section.

5.2.1 MODIFICATION INTO THE ORIGINAL MODEL

The equation 3.11 (Section 3.1) was originally written as follows in the software code:

$$v = M + 2e \sin M + \frac{5}{4}e^2 \cos M \quad (5.1)$$

Using the equation below instead of Equation 3.11 to perform the error analysis resulted in the following figures (Fig. 5.6, 5.7 and 5.8). Comparing Figure 5.6 to Figures 5.2 and 5.3, it is possible to verify that the model using Equation 5.1 provides a different result. Moreover, Figures 5.7 and 5.8 provides a wide range of angle error. These observations led to a deep analysis into the original model, and consequently a mistake was found into the code. The true anomaly is written as Equation 3.10:

$$v = M + \left(2e - \frac{1}{4}e^3\right) \sin M + \frac{5}{4}e^2 \sin 2M + \frac{13}{12}e^3 \sin 3M \quad (5.2)$$

Comparing equations 5.1 and 5.2, it is possible to verify the original model was using **cos M** instead of **sin 2M**. Therefore, the mistake was corrected and the error analysis was performed according to Section 5.1.

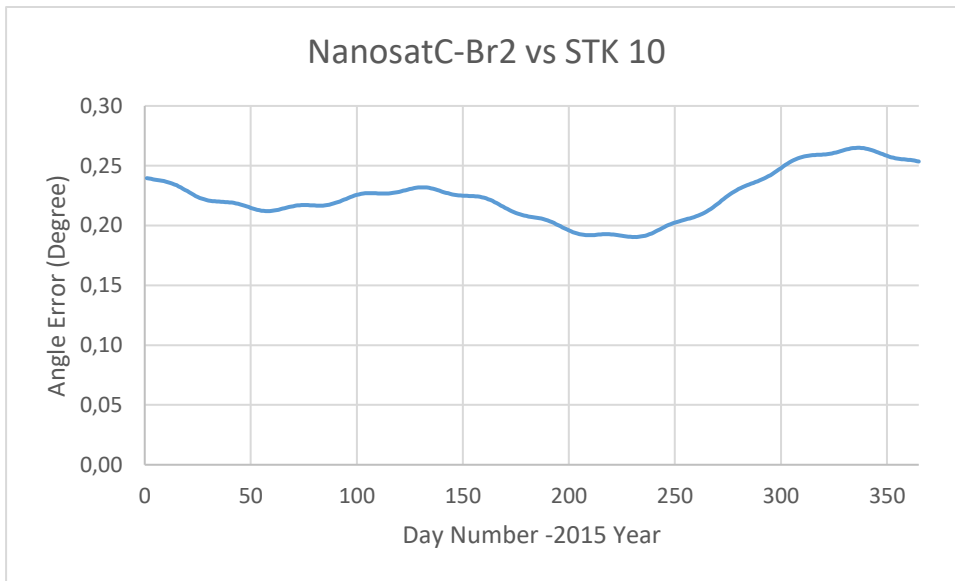


Figure 5.6 – Behavior of NanoSatC-Br2 in comparison with STK 10

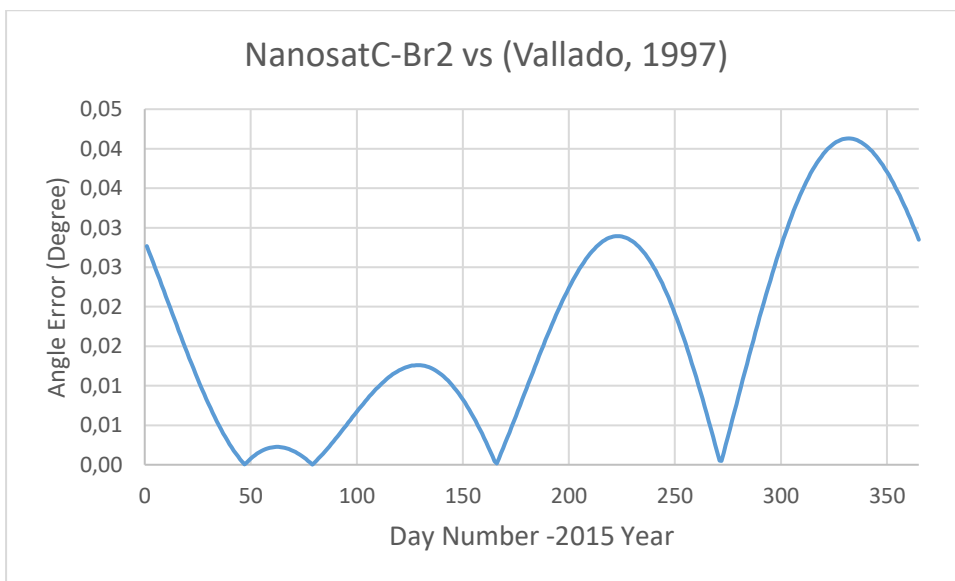


Figure 5.7 – Behavior of original model in comparison with Vallado's Model

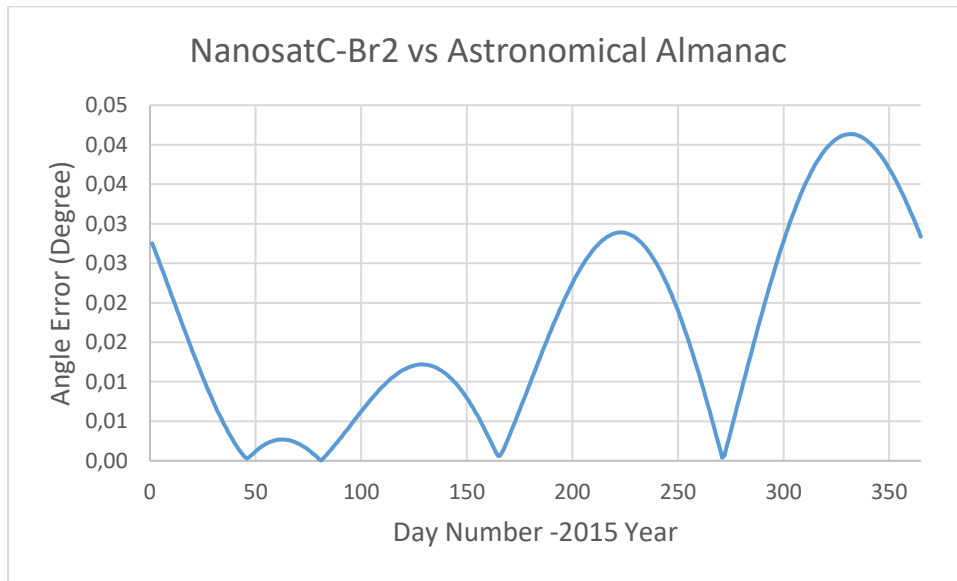


Figure 5.8 – Behavior of the original model in comparison with Astronomical Almanac 2015 model

5.2 ERROR ANALYSIS: MAGNETIC FIELD VECTOR

The attitude determination software of NanoSatC-BR2 utilizes the IGRF12 model to determine the magnetic field vector. However, this model is truncated, leading to a code which performs less calculations in comparison to the original model. The inputs of the code are the year fraction, the colatitude (0-180°), the east longitude (0-360°) and the radial distance from the center of the Earth (km).

Two types of analyses were made, and the results of both will be presented in this work. The first analysis takes into consideration all possible combinations of colatitude and east longitude, and a fixed value of year fraction (2015.5) and of radial distance (7000 km). The radial distance was set to 7000 km to simulate the real radial distance of a nanosatellite. For example, the average radial distance of the NanosatC-Br1 during the 2015 year was 6985 km, according to STK 10.

The second analysis was based on real inputs of the NanosatC-Br1, provided by STK 10, during the year of 2015. This software provided the colatitude, east longitude and radial distance of the NanosatC-BR1 of each day of the 2015 year.

The results of these two analyses are presented in Table 5.8. It is possible to verify that the results of both analyses are approximated. For example, the Average Absolute Magnitude Error of the first analysis is 0.50%, while the Average Absolute Magnitude Error of the second

analysis is 0.62%. These results shows that the difference between the magnitude of the truncated model and the IGRF12 is small.

Table 5.8 – Error Analysis Results: Comparison Between the Analyses

Type of Errors	Analysis 1	Analysis 2
Max. Absolute Magnitude Error (%)	2.80	3.10
Min. Absolute Magnitude Error (%)	0.03	0.00
Average Absolute Magnitude Error (%)	0.50	0.62
Maximum Angle Error (Deg)	1.60	1.53
Minimum Angle Error (Deg)	0.03	0.01
Average Angle Error (Deg)	0.50	0.42
Standard Deviation of Angle Error	3.09E-01	2.66E-01

Moreover, Table 5.8 presents values of angle errors, which also shows that the difference between both models is small. For example, Analysis 1 provided an average angle error of 0.5°, whereas the Analysis 2 provides an average angle error of 0.42°.

Ghuffar (2010) also compared the original IGRF12 and the IGRF12 truncated for $n=m=5$, and the results are similar to the results presented in Table 5.8. For example, the Maximum Magnitude Error (%), Maximum Error Angle (degree) and Average Error Angle (degree) is 3.42%, 1.48° and 0.42°, respectively.

Figures 5.6 and 5.7 presents the histogram of Frequency of Magnitude Error versus Magnitude Error. The results of both figures shows that low values of magnitude errors occur more frequently than the magnitude errors of high values (negative or positive).

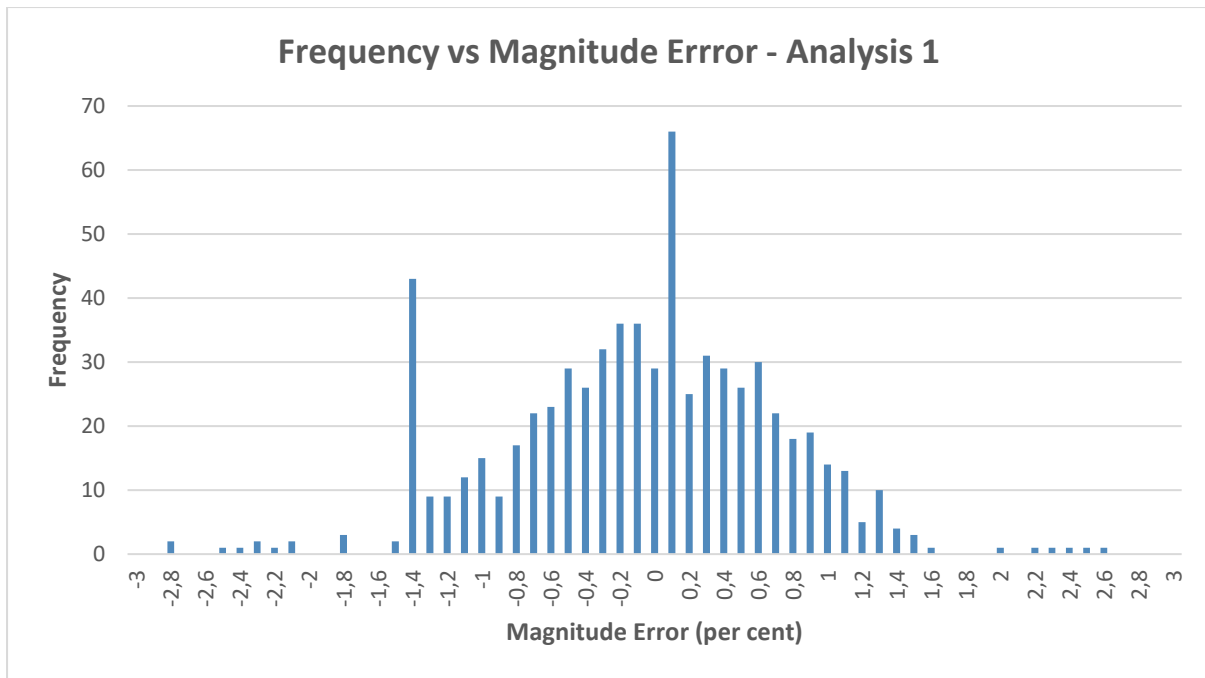


Figure 5.5 – Histogram Frequency vs Magnitude Error for Analysis 1

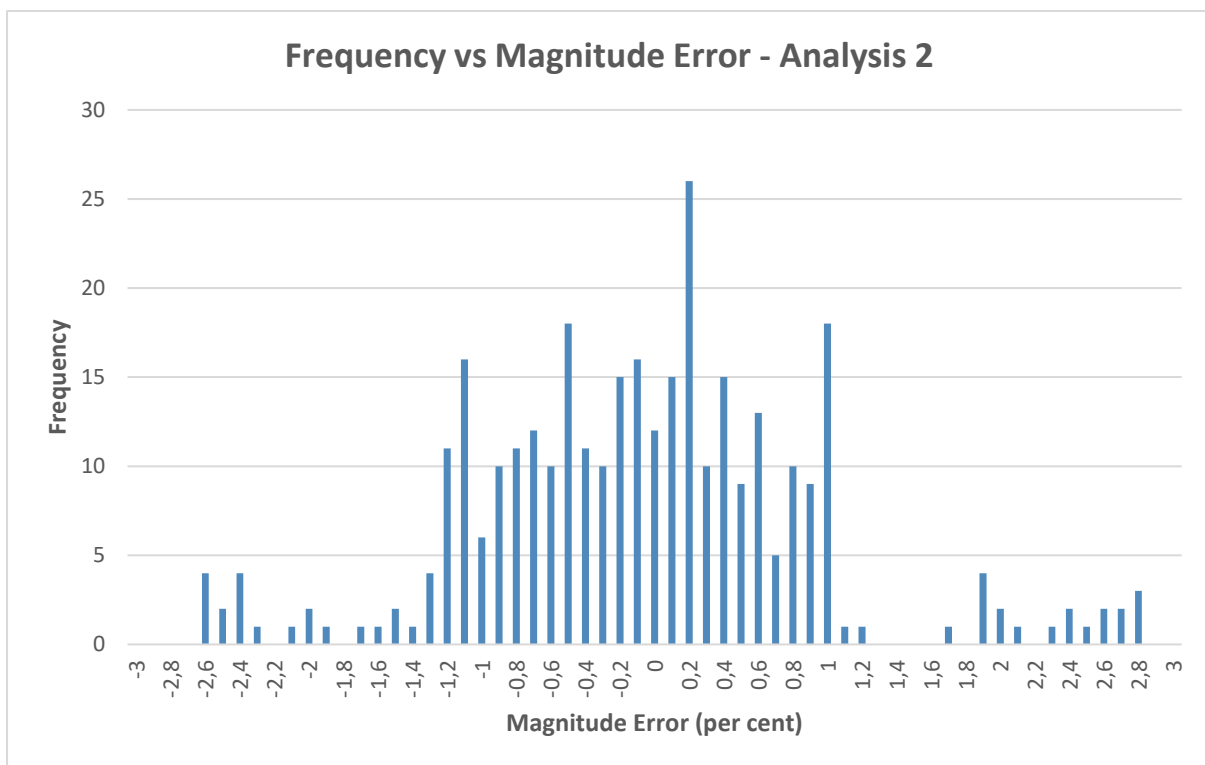


Figure 5.6 – Histogram Frequency vs Magnitude Error for Analysis 2

In brief, the simulation of the truncated provided acceptable results compared to the original model.

6 SCHEDULE OF ACTIVITIES

The schedule of activities is presented as follows:

Table 6.1 – Schedule of Activities

TASK	TG I			TG II			TG III		
	M 1	M 2	M 3	M 1	M 2	M 3	M 1	M 2	M 3
Topic Familiarization (papers, books, etc.)	X	X	X						
Introduction, Methodology, Schedule of Activities	X	X	X						
Preparation of report (TG I)		X	X						
Literature Review				X					
Familiarization to the attitude det. software				X	X	X	X		
Preparation of report (TG II)					X	X			
Results and Discussion						X	X	X	

Preparation of final dissertation (TG III)							X	X	
Preparing for dissertation defense (Presentation)							X	X	

Where M means Month.

7 CONCLUSIONS

Throughout the development of this dissertation, the student could study the necessary steps performed to determine the attitude of a satellite in terms of quaternions, therefore this work was important to familiarize the student to the topic, and enable the student to examine the big picture of what happens inside of a real attitude determination system. For example, the student was able to understand the interfaces of the system, such as the mathematical models to determine the vectors in the inertial frame.

The three simulations obtained expected rotation matrices using the quaternions provided by the software, which means QUEST algorithm of the system is working accordingly.

In addition, the results of the error analysis between the NanosatC-Br2's model to determine the sun position vector and low precision models such as the Vallado's model and the Astronomical Almanac model provided small average angle error and maximum angle error. This result is expected once the three models are low precision models. On the other hand, these models, when compared to the results provided by the STK, resulted in higher average angle errors and maximum angle errors. As the STK is "black box" once it is not possible to know which model it is using to determine the sun position vector, it is possible to conclude that this software may use a model with higher or low precision compared to the other three models. However, the sun position vectors in the inertial frame provided an average angle

error lower than 1° , and the average magnitude error was approximately 1% in comparison with the two models found in literature, and in comparison with STK results.

Finally, the truncated IGRF12 model ($n=m=5$) has the advantage to perform less calculations in comparison to the original IGRF12 ($n=m=13$), and even so the average absolute magnitude errors between these two models are considered small, that is, it is 0.5% for the Analysis 1 and 0.62% for the Analysis 2. In addition, the obtained Average Angle Error between these two models is 0.5° for the Analysis 1 and 0.42° for the Analysis 2. Therefore, the magnetic field vector in the inertial frame determined using $n=m=5$ provided average angle errors and average magnitude errors lower than 1° and 1%, respectively, when compared with the original model ($n=m=13$).

REFERENCES

- AGI (2015). STK. Retrieved from <http://www.agi.com/products/stk/> [Accessed: Jan 25, 2015]
- Bureau International des Poids et Mesures (2014). ***“SI Brochure: The International System of Units (SI)”***. France: 8th Edition. Retrieved from <http://www.bipm.org/en/publications/si-brochure/second.html> [Accessed: June 04, 2016]
- British Geological Survey (2014). ***IGRF (12th Generation, revised 2014) Synthesis Form***. Retrieved from http://www.geomag.bgs.ac.uk/data_service/models_compass/igrf_form.shtml [Accessed: Jan 25, 2015]
- Carvalho, Ricardo José de. (2008). ***Times Scales, UT0, UT1, EAL, TAI, UTC***. U.S. National Observatory: Time Service Division. Retrieved from https://tf.nist.gov/sim/2008_Seminar/TimeScales003.ppt [Accessed: June 04, 2016]
- Castro, João Carlos Vilela de. (2006) ***Desenvolvimento de um Dispositivo para Determinação de Atitude de Satélites Artificiais Baseado em Magnetômetro de Estado Sólido***. (Bachelor dissertation in Automation and Control Engineering). Universidade Federal de Ouro Preto, Ouro Preto.
- Chauhan, J. P. (2008). ***Space Dynamics for Graduate Students***. India: Krishna Prakashan Media.
- Cheng, Yang; Shuster, Malcom D. (2008). ***Speed Testing of Attitude Estimation Algorithms***. The Journal of Astronautical Sciences, JAS- 1294.
- Crassidis, John L.; Markley, F. Landis. (1997) ***A Predictive Attitude Determination Algorithm***. Proceedings of the Flight Mechanics/Estimation Theory Symposium, Greenbelt, MD: NASA-Goddard Space Flight Center. pp. 249-263.
- Crassidis, John L.; Markley, F. Landis. (2014). ***Fundamentals of Spacecraft Attitude Determination and Control***. New York, USA: Springer.
- CubeSat Design Specification (CDS). (2014). California Polytechnic State University, SLO. Rev. 13.
- Curtis, Howard D. (2014). ***Orbital Mechanics for Engineering Students***. Third Edition. United States: Elsevier.
- Defense Dept. Naval Observatory. (2014). Astronomical Almanac for the year 2015. Nautical Almanac Office.

- Duarte, Ricardo O.; Martins-Filho, Luiz; Kuga, Hélio K. (2009). *Performance Comparison of Attitude Determination Algorithms Developed to Run in a Microprocessor*. 20th International Congress of Mechanical Engineering. Gramado, RS, Brazil. November 15-20, 2009.
- Durão, Otávio C. S.; Essado, Marcelo. (2014). *Programa NanosatC-BR – Desenvolvimento de Cubesats*. 1º Convenção Nacional de Radioamadorismo, outubro, 2014.
- Fisher, Rick. (2006). *Astronomical Times*. National Radio Astronomy Observatory, US.
Retrieved from <https://www.cv.nrao.edu/~rfisher/Ephemerides/times.html> [Accessed: Jan. 11, 2016]
- Fitzpatrick, Richard. (2010). *A Modern Almagest. An Updated Version of Ptolemy's Model of the Solar System*. The University of Texas at Austin. Retrieved from <https://farside.ph.utexas.edu/books/Syntaxis/Almagest/> [Accessed: May 29, 2016]
- Ghuffar, Sajid. (2010). *Design and Implementation of a Attitude Determination Algorithm for the Cubesat UWE-3* (Msc, Thesis in Space and Technology). Julius-Maximilians-Universität Würzburg, Würzburg, Germany and Luleå University of Technology, Luleå, Sweden.
- Hall, Chris (2003). *Introduction to Attitude Dynamics and Control*. Virginia Tech, 2003.
Retrieved from <http://www.dept.aoe.vt.edu/~cdhall/courses/aoe4140/intro2adcs.pdf> [Accessed: March 2, 2015]
- Hall D., Christopher. (2003). *Spacecraft Attitude Dynamics and Control*. Virginia Tech,
Retrieved from Lecture Notes Online Web site: <http://www.dept.aoe.vt.edu/~cdhall/courses/aoe4984/page4.html>
- Holbert, Keith E (2006). Single Event Effects. EEE 598 – Radiation Effects course. Arizona State University. Retrieved from <http://holbert.faculty.asu.edu/eee560/see.html> [Accessed: July 11, 2016]
- Hoots, Felix R. and Roehrich, Ronald. L. (1980) “Spacetrack Report No. 3 – Models for Propagation of NORAD Element Sets”. U.S. Air Force Aerospace Defense Command, Colorado Springs, CO. Retrieved from <https://celestrak.com/NORAD/documentation/spacetrk.pdf> [Accessed: June 12, 2016].
- INPE (2015). NANOSATC-BR. Website. Disponível em: <http://www.inpe.br/crs/nanosat/index.php> [Accessed: March 1, 2015].

- Maini, Anil K.; Agrawal, Varsha (2014). *Satellite Technology, Principles and Applications*. 3rd Edition. India: John Wiley & Sons.
- Markley, Landis F.; Mortari, Daniele. (1999) *How to Estimate Attitude from Vector Observations*. ASS Paper 99-427, presented at the AAS/AIAA Astrodynamics Specialist Conference. Girdwood, Alaska, August 16-19, 1999.
- Markley, Landis F (1998) *Attitude Determination Using Two Vectors Measurements*. Guidance, Navigation, and Control Systems Engineering Branch, Code 571. NASA's Goddard Space Flight Center, Greenbelt, MD 20771.
- Marques, Sónia Maria Martinho (2000). *Small Satellites Attitude Determination Methods*. (Msc, Thesis in Computer and Electronic Engineering). Universidade Técnica de Lisboa. Instituto Superior Técnico. Lisboa: Dezembro, 2000.
- Martin, Andrea. (2013). *Two Cubesat Technology Demonstrations Launch in December*. NASA Website. Retrieved from http://esto.nasa.gov/news/news_CubeSats_12_2013.html [Accessed: March 22, 2015].
- Murad, A. H.; Jang K. D.; Atallah G.; Karne R.; Baras, J. (1995). *Technical Research Report. A Summary of Satellite Orbit Related Calculations*. The Center for Satellite and Hybrid Communication Networks - University of Maryland.
- NASA (2011). *Definition of Two-line Element Set Coordinate System*. Retrieved from http://spaceflight.nasa.gov/realdata/sightings/SSapplications/Post/JavaSSOP/SSOP_Help/tle_def.html [Accessed: June 12, 2016].
- National Institute of Standards and Technology (n.d.). "Frequently asked question (FAQ)." NIST, Maryland, USA. [Online]. Available: http://www.nist.gov/public_affairs/contact.cfm [Accessed: June 04, 2016].
- Normand, Eugene. (2008). Single Event Effects in Avionics. Boeing Radiation Effects Lab. Retrieved from <http://www.solarstorms.org/SEUavionics.pdf> [Accessed: June 04, 2016].
- Schlyter, Paul. (n.d.) *How to compute planetary positions*. Retrieved from <http://stjarnhimlen.se/comp/ppcomp.html> [Accessed: Nov. 29, 2015].
- Schlyter, Paul (2010). *Time Scales*. Retrieved from <http://stjarnhimlen.se/comp/time.html> [Accessed: Jan. 25, 2016].
- Seago, H. John, and Seidelmann, Kenneth P. (2013) "*The Mean-Solar-Time Origin of Universal Time and UTC*." in Advances in the Astronautical Sciences, Volume 148. USA: American Astronautical Society, 2013. pp. 486. Retrieved from

- http://www.agi.com/downloads/resources/white-papers/AAS_13-486.pdf [Accessed: May 21, 2016].
- Sellers, Jerry J. Understanding Space. (2004). *An Introduction to Astronautics*. Revised Second Edition. 2004. USA; Mcgraw Hill.
- Shuster, M. D. (1978). *Approximate Algorithms for Fast Optimal Attitude Computation*, Paper AIAA 78-1249, Proceedings, AIAA Guidance and Control Conference, Palo Alto, California, August 7-9, 1978, pp. 88-95.
- Shuster, M. D. and Oh, S. D. (1981). "Three-Axis Attitude Determination from Vector Observations", Journal of Guidance and Control, Vol. 4, No. 1, January-February 1981, pp. 70-77.
- Sumus Technology (2016). Two-line element (TLE) format. Retrieved from <http://www.stltracker.com/resources/tle>
- Thébault, Erwan, et al. (2015). *International Geomagnetic Reference Field: the 12th generation*. Earth, Planets and Space, 67 (79). Springer, 2015. Retrieved from <http://www.earth-planets-space.com/content/pdf/s40623-015-0228-9.pdf> [Accessed: Jan. 24, 2016].
- Vallado, David A. (1997) *Fundamentals of Astrodynamics and Applications*. Space Technologies Series. United States of America: Mcgraw-Hill.
- Wertz, James R. (2002). *Spacecraft Attitude Determination and Control*. Dordrecht: D. Reidel Publishing Company.
- Weston, Harley. (n.d.). A note on standard deviation. University of Regina, Department of Mathematics and Statistics. Retrieved from Lecture Notes Online Web site: <http://mathcentral.uregina.ca/RR/database/RR.09.95/weston2.html>